Highly Efficient Bayesian Updating using System Reliability Methods with Metamodels: An Adaptive Kriging-Based Approach

2 3 4

1

Zeyu Wang, Abdollah Shafieezadeh

5 6

7

8

9

10

11

12

13

14

15

16

17

18

19

20

21

22

23

24

25

26

27

28

29

Department of Civil, Environment and Geodetic Engineering, The Ohio State University, Columbus, OH

ABSTRACT

Bayesian updating offers a powerful tool for probabilistic calibration and uncertainty quantification of models as new observations become available. By reformulating Bayesian updating into a reliability problem via introducing an auxiliary random variable, the state-of-the-art Bayesian updating with structural reliability method (BUS) has showcased large potential to achieve higher accuracy and efficiency compared with conventional approaches based on Markov Chain Monte Carlo simulations. However, BUS faces a number of limitations. The transformed reliability problem often involves a very rare event especially when the number of observations increases. This along with the fact that conventional reliability analysis techniques are not efficient, and often not capable of accurately estimating the probability of rare events, unavoidably lead to a very large number of evaluations of the likelihood function and simultaneously insufficient accuracy of the derived posterior distributions. To overcome these limitations, we propose Simple Rejection Sampling with Multiple Auxiliary Random Variables (SRS-MARV), where the limit state function in BUS is decomposed into a system reliability problem with multiple limit state functions. The main advantage of this approach is that the acceptance rate of each decomposed limit state function is significantly improved, which facilitates effective integration of adaptive Kriging-based reliability analysis into SRS-MARV. Moreover, a new stopping criterion is proposed for efficient, adaptive training of the Kriging model. The proposed method called BUAK is shown to be highly computationally efficient and accurate based on results of comprehensive investigations for three diverse benchmark problems. Compared to the state-of-the-art methods, BUAK substantially reduces the computational demand by one to three orders of magnitude, therefore, facilitating the application of Bayesian updating to computationally very intensive models.

Key words: Bayesian Updating; Bayesian Inference; Calibration; Reliability Analysis; Kriging; MCMC

1. Introduction

1

2

3

4

5

6

7

8

9

10

11

12

13

14

15

16

17

18

19

20

21

22

23

24

25

26

Recent advancements in inspection and monitoring techniques for various applications such as structural and infrastructure systems offer unprecedented capabilities to improve design, planning and management of these systems. Information obtained via such observations can be leveraged to update probabilistic or stochastic representations of uncertainties in models to better support risk-informed decision-making. Upto-date information on responses and features including, for example, system capacities, structural deformations, system dynamic features and deteriorations assist in comprehensively perceiving the probabilistic information of system variables. A well-established method for this purpose is Bayesian updating that derives the posterior probabilistic information from the often empirically defined prior statistical assumptions and new observations.

In the past, the posterior distribution has commonly been estimated through the implementation of Markov chain Monte Carlo (MCMC) simulation [1]. Some other approximation-based approaches such as Laplace approximation method [2] have also shown good performance in terms of computational efficiency. However, they may yield inaccurate results especially when the number of random variables or the complexity of the posterior density increase [3]. In the MCMC-based Bayesian updating approach, random realizations are generated by the proposal function, whose mean value changes in relation to the last accepted realization. The samples generated by the proposal function are then compared with a random value drawn from the standard uniform distribution to determine whether those points should be accepted or rejected. It has been shown that the probability density of the accumulated accepted points converges to the posterior density. However, lack of guarantee to converge to a stationary state corresponding to Markov chain is the major limitation of the MCMC-based Bayesian updating method [3]-[5]. To address this limitation, the transitional Markov chain Monte Carlo simulation (TMCMC) has been proposed by Ching et al. [6], which attempts to adaptively sample from a series of intermediate probability distributions and transitionally converge to the target posterior probability distribution. Although, the TMCMC-based Bayesian updating method improves the performance by avoiding the burn-in phenomena in the conventional approach, the gained efficiency is not significant when the dimension of the variable space

increases [3], [7]. As an alternative, Straub and Papaioannou [4] proposed a new method called Bayesian Updating with Structural reliability methods (BUS). The primary idea behind BUS is reformulating Bayesian updating problems into structural reliability problems. By introducing an auxiliary standard uniform random variable P, the Bayesian updating problem with simple rejection sampling strategy targets realizations that satisfy the limit state equation: $p \le cL(x)$, where c is a constant ensuring the maxima of cL(x) is smaller than one. Based on this formulation, the problem of Bayesian updating is transformed into a structural reliability problem with corresponding random variables [X, P] with the aim changed to finding the failure points. By avoiding the process for ensuring the stationarity of Markov Chain in MCMC, BUS applies the subset simulation technique [8], [9] to focus on the accepted domain regardless of the dimension of random variables. This method adaptively approaches the failure domain through sequentially sampling a series of nested intermediate domains until the target number of samples for deriving posterior distributions are obtained. BUS has shown great efficiency in estimating posterior distributions using subset simulation techniques [10]–[12]. However, the process of estimating the posterior distribution through BUS with subset simulation is computationally expensive, especially when the likelihood functions become very complex e.g. when they involve time-consuming computational models [3], [5]. This is in part due to the use of subset simulation method for solving the structural reliability problem in BUS, which requires a large number of evaluations of the performance function. Second, as the shape of the limit state function for BUS in the standard normal space is typically highly nonlinear, methods such as First and Second Order Reliability Methods (FORM & SORM) may become very inaccurate. This challenge is compounded as the number of observations increases. The resulting high computational demand can be overcome through the application of surrogate model-based reliability analysis methods. The surrogate models can include Response Surface [12]-[14], artificial neural networks [3], Polynomial Chaos Expansion [15], Support Vector Regression [16], [17], and Kriging [18]–[21]. Among these methods, adaptive Kriging-based reliability analysis methods have been shown to be one of the most accurate and efficient methods in solving reliability problems [18], [22]–[24], and therefore have gained significant attention in recent years [25], [26]. However, the failure probability

1

2

3

4

5

6

7

8

9

10

11

12

13

14

15

16

17

18

19

20

21

22

23

24

25

associated with the acceptance ratio in BUS is significantly small and can reach 10^{-6} or even smaller as the number of observations increases. Such levels of failure probability are quite challenging to estimate for reliability analysis techniques using limited number of function evaluations. To apply adaptive Krigingbased reliability analysis methods here, the number of candidate design samples should be extremely large to ensure a well-trained Kriging surrogate model [18] that can yield accurate estimates of these very small failure probabilities. In such a circumstance, the implementation of adaptive Kriging-based reliability analysis methods in conjunction with BUS becomes extremely computationally inefficient, if not infeasible. In this paper, we propose a method called Bayesian Updating using Adaptive Kriging (BUAK) to address the above issues. In BUAK, the component structural reliability analysis problem in BUS is transformed to a system reliability analysis problem, which facilitates the implementing of adaptive Kriging-based reliability analysis methods. Unlike the approach in BUS that uses only one auxiliary standard uniform random variable, we introduce multiple auxiliary standard uniform random variables to decompose the component structural reliability problem in BUS into a parallel system reliability problem with multiple limit state functions. This approach yields the same outcome in terms of the probability of failure corresponding to the acceptance ratio as the one in BUS, however, each component limit state function in BUAK does no longer correspond to a rare event. This development means that the corresponding limit state functions can be efficiently substituted by Kriging surrogate models through the adaptive Kriging-based structural reliability analysis methods. Therefore, the number of evaluations of the likelihood function significantly reduces, while the posterior probability distributions are estimated accurately. Eventually, with the well-trained Kriging surrogate model, samples with posterior distribution can be generated unlimitedly, as this process will no longer rely on the computationally expensive likelihood function. In the rest of this paper, Bayesian updating and BUS method are briefly introduced in Section 2. Methods derived based on system reliability analysis and their integration into Bayesian updating framework are represented in Section 3. Section 4 presents the Bayesian updating method based on adaptive Kriging, which is referred to as BUAK. Three numerical examples selected from literature are used to

1

2

3

4

5

6

7

8

9

10

11

12

13

14

15

16

17

18

19

20

21

22

23

24

25

analyze the performance of *BUAK* in Section 5. Conclusions are drawn in Section 6.

2. Bayesian Updating

Due to technical difficulties or high costs associated with direct observations of some of key properties of natural or built systems, their status is often inferred by taking reference to observations of other auxiliary variables that are easy to measure. For instance, natural frequencies of a building can implicitly reflect its inter-story stiffness [4], and such frequencies can be derived from ambient vibrations measured via cheap accelerometers. Generally, as the number of observations increases, the uncertainties of those parameters decreases. Bayesian updating facilitates the uncertainty reduction using the likelihood of observed properties and assuming a reasonable prior probability distribution for unknown parameters (i.e., inter-story stiffness in the building example) denoted as f'(x) based on empirical knowledge, and then estimating the posterior probability distribution denoted as f'(x) can be estimated by the Bayes' theorem:

$$f'(x) = \frac{L(x)f(x)}{\int_{\Omega} L(x)f(x)dx}$$
 (1)

where Ω is the probabilistic domain of random variable x and L(x) is the so-called likelihood function, which is proportional to the conditional probability of observations given a parameter state, and can be expressed as:

$$L(\mathbf{x}) \propto \Pr(Z|\mathbf{X} = \mathbf{x}) \tag{2}$$

In estimating f'(x) through MCMC, the denominator $\int_{\Omega} L(x)f(x)dx$ in Eq. (1) can be ignored since it is only a normalizing constant ensuring that f'(x) integrates to one. Typically, the likelihood function L(x) is composed of three parts: observations Z, responses from the model s(x) and error ε that represents the deviation of s(x) from Z. Because of measuring and modeling errors, observations Z can not perfectly reflect s(x). The associated error can be represented as follows:

$$\varepsilon = Z - s(x) \tag{3}$$

- 1 Note that the error in Eq.(3) is often defined through a multiplicative error term, especially when the error
- stems from the modeling uncertainty as suggested in [4]. Generally L(x) can be estimated through the
- 3 probability density function (PDF) of the error ε as:

$$L(\mathbf{x}) = \rho_{\varepsilon}(\varepsilon) = \rho_{\varepsilon}(Z - s(\mathbf{x})) \tag{4}$$

- where $\rho_{\varepsilon}(\cdot)$ denotes the PDF of ε . Although the type of the PDF of L(x) is commonly considered to be
- 6 multivariate Gaussian distribution with zero mean, it can be any other unbiased distribution. When m
- 7 mutually independent observations are available, the likelihood function in Eq. (4) can be presented as:

$$L(\mathbf{x}) = \prod_{i=1}^{m} L_i(\mathbf{x}) = \prod_{i=1}^{m} \rho_{\varepsilon_i} (Z_i - s_i(\mathbf{x}))$$
 (5)

9 In this article, the likelihood function is denoted as L(x) for both independent and dependent observations.

2.1 Simple Rejection Sampling (SRS)

- 11 The idea of transforming Bayesian updating problems into structural reliability problems according to the
- simple rejection algorithm was initially proposed by Straub and Papaioannou [4]. It is known that the goal
- of Bayesian updating is to estimate the posterior distribution f'(x), which is proportional to the product of
- the likelihood L(x) and prior distribution f(x):

$$f'(x) \propto L(x)f(x) \tag{6}$$

- For the estimation of f'(x), the use of the conventional MCMC approach, which requires ensuring the
- 17 stability of the Markov Chain, is not computationally efficient. Simple rejection sampling algorithm can be
- applied here to overcome this limitation. First, the accepted domain Ω_{acc} can be defined corresponding to
- the augmented outcome space [x, p] with an auxiliary random variable P expressed as:

$$\Omega_{acc} = [p \le cL(\mathbf{x})] = [h(\mathbf{x}, p) \le 0] \tag{7}$$

- where h(x, p) = p cL(x) and c is a constant satisfying $cL(x) \le 1$ for all the outcomes from X.
- Therefore, *c* can be defined as:

$$c = \frac{1}{max(L(x))} \tag{8}$$

- The strategy of defining c in Eq.(8) is in fact the optimal one among all the feasible definitions. However,
- 2 it is not the only one and any definition that satisfies $cL(x) \le 1$ is applicable. Larger c leads to higher
- 3 acceptance rate [4]. Moreover, an adaptive approach to search for c is available in [5] and a method that
- 4 corrects the samples for the case where $cL(x) \le 1$ is discussed in [27]. In this research, the strategy in
- 5 Eq.(8) is adopted. Subsequently, the posterior distribution f'(x) can be formulated as:

$$f'(\mathbf{x}) = \frac{\int_{p \in \Omega_{acc}} f(\mathbf{x}) dp}{\int_{[\mathbf{x}, p] \in \Omega_{acc}} f(\mathbf{x}) dp d\mathbf{x}} = \frac{\int_0^1 I^{acc}([\mathbf{x}, p] \in \Omega_{acc}) f(\mathbf{x}) dp}{\int_{\mathbf{x}} \int_0^1 I^{acc}([\mathbf{x}, p] \in \Omega_{acc}) f(\mathbf{x}) dp d\mathbf{x}}$$
(9)

- 7 where $I^{acc}([x,p] \in \Omega_{acc})$ is the indicator function corresponding to the structural reliability problem with
- 8 the limit state function h(x,p) = p cL(x). The numerator and denominator in Eq. (9) can be easily
- 9 extended as:

10
$$\int_0^1 I^{acc}([\mathbf{x}, p] \in \Omega_{acc}) f(\mathbf{x}) dp = \int_0^{cL(\mathbf{x})} f(\mathbf{x}) dp = cL(\mathbf{x}) f(\mathbf{x})$$
 (10)

11 and

$$\int_{X} \int_{0}^{1} I^{acc}([x,p] \in \Omega_{acc}) f(x) dp dx =$$

$$\int_{X} \left\{ \int_{0}^{1} I^{acc} \left(p \le cL(x) \right) dp \right\} f(x) dx = \int_{X} cL(x) f(x) dx \tag{11}$$

- 13 Equations (10) and (11) are exactly the same as the numerator and denominator of Eq. (1), respectively.
- 14 Therefore, a simple rejection sampling algorithm is available according to [28], which is presented in
- Algorithm 1. However, the simple rejection sampling algorithm faces the limitation that the acceptance rate
- significantly decreases as the number of observations m increases. Straub and Papaioannou [4] showed that
- 17 the average acceptance rate is proportional to $\frac{1}{\sqrt{m}}$, when all measurements are independent and identically
- distributed (iid). This limitation makes the process of Bayesian updating computationally intractable since
- 19 very few accepted points can be generated to estimate the posterior distribution, while a very large number
- 20 of unnecessary points are generated. This issue becomes especially problematic when costly experimental
- or computational models are involved.

Algorithm 1. Simple Rejection Sampling

- 1. i = 1
- 2. Generate a sample x^i from f(x)
- 3. Generate a sample p^i from the standard uniform distribution [0.1]
- 4. If $[\mathbf{x}^i, p^i] \in \Omega_{acc}$
 - (a). Accept x^i
 - (b). i = i + 1
- 5. Stop if $i = N_s$, else go to step 2

1 2

2.2 Bayesian Updating with Structural Reliability Methods (BUS)

- 3 Due to the inherent limitation of simple rejection sampling method with regard to its low acceptance rate,
- 4 the MCMC method was proposed for Bayesian updating. However, to ensure a stable Markov chain, the
- 5 MCMC-based Bayesian updating needs to investigate still a very large number of evaluations of the
- 6 likelihood function. On the other hand, although the acceptance rate of simple rejection sampling-based
- 7 Bayesian updating approach is low, it is very straightforward to implement and it can guarantee accurate
- 8 posterior distributed samples. To maintain those advantages of the simple rejection-based approach, Straub
- 9 and Papaioannou [4] proposed Bayesian Updating with Structural Reliability Methods (BUS) by
- strategically integrating the simple rejection sampling approach with structural reliability analysis methods.
- In BUS, the Bayesian updating problem is handled in a way that involves solving a reliability analysis
- problem. The equivalent limit state function in BUS approach is defined as:

$$h(x,p) = p - cL(x) \tag{12}$$

- Note that the task of Bayesian updating is different from that in reliability analysis. In the process of
- reliability analysis, the target is to estimate the probability of failure, while drawing samples in the accepted
- 16 (failure) domain is the main purpose of BUS. Concerning this point, many existing reliability analysis
- 17 methods such as First & Second Order Reliability Methods (FORM & SORM), Importance Sampling (IS)
- and subset simulation (SS) should be adjusted to be applicable in association with BUS. For instance, the
- 19 combination of subset simulation and BUS has shown great efficiency in drawing samples from posterior
- distributions. Details of BUS with subset simulation haven been shown in Algorithm 2. However, BUS
- 21 algorithm also faces a number of challenges. As noted earlier, the acceptance rate in simple rejection

sampling approach tends to be extremely small when the number of observations increases. In this circumstance, the estimation of posterior distributions is equivalent to the analysis of reliability of rare events, which becomes rather computationally expensive for simulation-based approaches including subset simulation. To elaborate this point, the number of subsets can be denoted as N_{ss} , thus the total number of evaluations of the likelihood function N_{call} can be determined as:

$$N_{call} = N_{ss} \cdot N_{in} + N_t - N_{ts} \tag{13}$$

where N_{in} is the number of samples in each intermediate subset, N_t is the number of final samples and N_{ts} is the number of seeds in the final subset. As indicated in Eq.(13), the computational cost, N_{call} , typically increases linearly with $-\log(p_{acc})$ and this is due to the fact that N_{ss} is proportional to $-\log(p_{acc})$. Note that N_{call} can easily reach thousands in BUS with subset simulation. Although this number is considerably smaller compared to the crude Monte Carlo simulation or MCMC, it is still computationally very inefficient for Bayesian updating for sophisticated computational models. Moreover, the limit state function h(x, p) can be highly nonlinear since h(x, p) includes an integrated likelihood function L(x), which contains the probability density function of Gaussian distribution. This may lead to inaccurate estimates of posterior distributions if approximation-based approaches such as FORM & SORM are used.

Kriging-based reliability analysis methods are known for their capabilities in substituting the limit state function through adaptive training of the surrogate models and thus reducing the number of evaluations of the performance function [18]. However, it is computationally inefficient to directly implement this approach in association with the limit state function in *BUS* (e.g. Eq. (12)). This is because with the increase in the number of observations, the acceptance ratio becomes small, which requires the number of candidate design samples to be extremely large. To address this challenge, we propose Simple Rejection Sampling with Multiple Auxiliary Random Variables (*SRS-MARV*), where the limit state function in Eq. (12) is decomposed into a series-system reliability problem with multiple limit state functions. A framework is subsequently proposed to integrate the Kriging-based reliability analysis method with *SRS-MARV*. The

- acceptance rate of each decomposed limit state function is relatively large, which enables the multiple
- 2 constructions of Kriging-based reliability analysis.

Algorithm 2. *BUS* with subset simulation

- 1. Define the parameters:
 - (a). Target number of samples N_t
 - (b). Number of samples in each intermediate step N_{in}
 - (c). Probability of intermediate subsets p_0
 - (d). Constant c according to the Eq. (8)
- 2. Draw N_{in} samples $[x_k, p_k]$, $k = 1, 2, ..., N_{in}$ from the prior distribution [X, P]
- 3. Define the subset domain such that $\Omega_1 = \{h(x, p) \le t_1\}$, where t_1 is defined according to the p_0 percentile of the responses of samples $h(x_k, p_k)$, $k = 1, 2, ... N_{in}$.
- 4. i = 1
- 5. While $t_i > 0$:
 - (a). i = i + 1
 - (b). Draw N_{in} samples from the domain Ω_{i-1} with MCMC technique
 - (c). Define the next subset $\Omega_i = \{h(x, p) \le t_i\}$, where t_i is defined according to the p_0 percentile of the responses of samples $h(x_k, p_k)$, $k = 1, 2, ..., N_{in}$ in subset Ω_{i-1}
- 6. Define the last subset $\Omega_{i+1} = \{h(x, p) \le 0\}$, identify the number of samples N_s in Ω_{i+1} and keep these samples as seeds
- 7. Draw N_t samples in the subset Ω_{i+1} with those seeds in Step 6 using MCMC technique
- S. Estimate the acceptance probability: $p_{acc} \approx p_0^i \cdot \left(\frac{N_s}{N_{in}}\right)$

4

5

3. Adaptive Kriging-based Reliability Analysis

- 6 The primary objective of using adaptive Kriging-based reliability analysis here is to train a surrogate model
- 7 $\hat{h}(x,p)$ to substitute the computationally demanding limit state function h(x,p) in Eq. (12). Then, SRS can
- 8 be applied directly on the computationally efficient surrogate model. In this section, the elements of the
- 9 Kriging model and Kriging-based reliability analysis are briefly reviewed. Then challenges of
- implementing adaptive Kriging-based reliability analysis methods are elaborated at the end of this section.
- 11 The Kriging surrogate model, also known as the Gaussian Process Regression, has been widely used in
- 12 computer-based experiment design [29]. In this model, the estimated responses follow a normal distribution
- parametrized by the mean values and variances [29], [30]. An extensive review of the Kriging surrogate
- model can be found in [18], [31]–[33]. In Kriging, the responses $\hat{h}(X)$ (X represents [X, P] in this section)
- are defined as:

$$\hat{h}(X) = F(\boldsymbol{\beta}, \boldsymbol{x}) + \psi(\boldsymbol{x}) = \boldsymbol{\beta}^T \boldsymbol{f}(\boldsymbol{x}) + \psi(\boldsymbol{x})$$
(14)

2 where **X** is the vector of random variables, $F(\beta, x)$ are the regression elements, and $\psi(x)$ is the Gaussian 3 process. In $F(\beta, x)$, f(x) is the Kriging basis and β is the corresponding set of coefficients. There are multiple formulations of $\boldsymbol{\beta}^T f(\boldsymbol{x})$ including ordinary (β_0) , linear $(\beta_0 + \sum_{i=1}^N \beta_i \boldsymbol{x}_i)$, or quadratic 4 $(\beta_0 + \sum_{i=1}^N \beta_i x_i + \sum_{i=1}^N \sum_{j=i}^N \beta_{ij} x_i x_j)$, where N is the number of dimensions of x. In this paper, the ordinary 5 6 Kriging model is used. The Gaussian process $\psi(x)$ has a zero mean and a covariance matrix that can be

7 represented as:

9

10

11

12

13

8
$$COV\left(\psi(\mathbf{x}_i), \psi(\mathbf{x}_j)\right) = \sigma^2 R\left(\mathbf{x}_i, \mathbf{x}_j; \boldsymbol{\theta}\right)$$
 (15)

where σ^2 is the process variance or the generalized mean square error (MSE) from the regression, computational detail of σ^2 is available in [34], x_i and x_j are two observations, and $R(x_i, x_j; \theta)$ is known as the kernel function representing the correlation between observations x_i and x_j parametrized by θ . The correlation functions implemented in Kriging can include, among others, linear, exponential, Gaussian, and Matérn functions. The Gaussian kernel function is used in this paper, which has the following form:

$$R(\boldsymbol{x}_i, \boldsymbol{x}_j; \boldsymbol{\theta}) = \prod_{k=1}^{N} \exp\left(-\theta^k (x_i^k - x_j^k)^2\right)$$
 (16)

where x_i^k is the kth dimension of x_i and θ is estimated via the Maximum Likelihood Estimation (MLE) 15 16 method [29]. It is shown that the variation of θ has significant impact on the performance of the Kriging meta-model [22], [35], [36]. To maintain consistency, θ^k is searched in $D_{\theta} = (0,10)$. Here, MLE can be 17 18 represented as:

19
$$\boldsymbol{\theta} = \underset{\boldsymbol{\theta}^* \in \mathcal{D}_{\boldsymbol{\theta}}}{\operatorname{argmin}} \left(\left| \boldsymbol{R}(\boldsymbol{x}_i, \boldsymbol{x}_j; \boldsymbol{\theta}^*) \right|^{\frac{1}{n_{tr}}} \sigma^2 \right)$$
 (17)

where $|R(x_i, x_j; \theta)|$ denotes the determinant of $R(x_i, x_j; \theta)$, n_{tr} is the number of training points and σ^2 is 20 the process variance defined in Eq.(15). Accordingly, the regression coefficient β , and the predicted mean 21 22 and variance can be determined as follows [29]:

23
$$\beta = (F^T R^{-1} F)^{-1} F^T R^{-1} Y$$

1 $\mu_{\widehat{h}}(x) = f^{T}(x)\beta + r^{T}(x)R^{-1}(y - F\beta)$

$$\sigma_{\widehat{h}}^{2}(x) = \sigma^{2}(1 - r^{T}(x)R^{-1}r(x) + (F^{T}R^{-1}r(x) - f(x))^{T}(F^{T}R^{-1}F)^{-1}(F^{T}R^{-1}r(x) - f(x)))$$
(18)

- where F is the matrix of the basis function f(x) evaluated at the training points, i.e., $F_{ij} = f_j(x_i)$, i =
- 4 1, 2, ..., n_{tr} ; j = 1, 2, ..., p, r(x) is the correlation between known training points x_i and an untried point x:
- 5 $r_i = R(x, x_i, \theta)$, $i = 1,2 \dots n_{tr}$, and **R** is the autocorrelation matrix for known training points: $R_{ij} =$
- 6 $R(x_i, x_j, \theta)$, $i = 1, 2, ..., n_{tr}; j = 1, 2, ..., n_{tr}$. Therefore, the estimated Kriging mean $\mu_{\hat{n}}(x)$ and
- 7 variance $\sigma_{\hat{h}}^2(x)$ can be presented as:

8
$$\hat{h}(\boldsymbol{u}) \sim N\left(\mu_{\hat{h}}(\boldsymbol{x}), \sigma_{\hat{h}}^2(\boldsymbol{x})\right)$$
 (19)

- 9 It is obvious that the responses from the Kriging model $\hat{h}(x)$ are not deterministic but probabilistic in the
- form of a normal distribution with mean $\mu_{\hat{h}}(x)$ and variance $\sigma_{\hat{h}}^2(x)$.
- 11 Kriging-based reliability analysis method is summarized in Algorithm 3. Note that learning functions
- have a crucial role in adaptive Kriging-based reliability analysis. As the name implies, the 'learning' refers
- 13 to the process of iterative selection of points for Kriging refinement based on the stochastic information for
- each design point. A popular learning function is U, which is concerned with uncertainties in the sign (\pm)
- estimation of $\hat{h}(x)=0$. In this regard, U takes the probabilistic distribution of estimated responses into
- 16 consideration, and quantifies the probability of making a wrong sign estimation in $\hat{h}(x)$. This learning
- function is used in this paper. The formulation of U is [18]:

$$U(\mathbf{x}) = \frac{|\mu_{\widehat{h}}(\mathbf{x})|}{\sigma_{\widehat{h}}(\mathbf{x})} \tag{20}$$

- In reliability analysis, the goal of learning function is often to identify points that have large variance and
- 19 close to the limit state $\hat{h}(x)=0$. Training the Kriging model this way enables accurate estimation of the sign
- of $\hat{h}(x)$ and therefore precise classification of accepted and rejected samples in Bayesian updating problems.

Algorithm 3. Adaptive Kriging-based Reliability Analysis

Draw N_{MCS} candidate design samples x_s , denoted as S, and initial training samples x_{tr} with Latin Hypercube Sampling technique (LHS)

- 2. Estimate the responses $h(x_{tr})$ of x_{tr} according to the performance function h
- 3. Construct the Kriging model \hat{h} according to training points x_{tr}
- 4. Estimate the $\mu_{\widehat{h}}(\mathbf{x})$, $\sigma_{\widehat{h}}^2(\mathbf{x})$, $U(\mathbf{x})$ and failure probability $\widehat{P}_f^{MCS} = \frac{\widehat{N}_f}{N_{MCS}}$ based on S with MCS, where \widehat{N}_f denotes the estimated number of failure samples Check if $min(U) \geq 2$ is satisfied or not:
- 5. (a). Satisfied. Go to step 6.
 - (b). Unsatisfied. Find the next best training point $x_{tr}^* = \arg\min_{x \in S} U(x)$ and go back to Step 2.
 - Check if $COV_{\hat{P}_f} \leq COV_{\text{thr}}$ is satisfied or not:
- 6. (a). Satisfied. Go to step 6.
 - (b). Unsatisfied. Update S by adding N_{Δ_S} extra candidate design points and go back to Step 4.
- 7. Output \hat{P}_f^{MCS}

The general principle of adaptive Kriging-based reliability analysis methods is to start with a small number of candidate design samples to estimate \hat{P}_f and then adaptively refine the model representing the limit state. To ensure that the number of candidate design samples N_{MCS} is sufficient, coefficient of variation of \hat{P}_f should satisfy:

$$COV_{\hat{P}_f} = \sqrt{\frac{1 - \hat{P}_f}{\hat{P}_f N_{MCS}}} \le COV_{\text{thr}}$$
 (21)

where \hat{P}_f is the estimated failure probability and COV_{thr} is the threshold for stopping criterion in step 6, 6 which is recommended to be 0.05 [18]. It is obvious that N_{MCS} influences COV_{P_f} , which means that the 7 final \hat{P}_f and the surrogate model for the limit state are reliable only when N_{MCS} is large enough to satisfy 8 $COV_{P_f} \leq COV_{\text{thr}}$. 9 10 A primary challenge in integrating adaptive Kriging-based reliability analysis with Bayesian updating here is to guarantee that N_{MCS} is sufficiently large when the number of observations in Eq. (5) increases. 11 The acceptance rate p_{acc} in Eq. (12) can be in the order of 10^{-8} or even smaller because of multiple 12 observations. For example, to satisfy $COV_{\hat{P}_f} \leq COV_{\text{thr}}$ in Eq. (21), N_{MCS} should be even greater than 13 4×10^{10} , which is computationally intractable. To overcome this challenge, we propose decomposing the 14 15 limit state function h into multiple limit state functions h_i , $i = 1, ... n_l$ with relatively large acceptance rates, where n_l is the number of decompositions of h. Then, n_l Kriging surrogate models \hat{h}_i , i=1,... n_l are 16

- 1 trained to substitute h_i . Subsequently, the integration of SRS and adaptive Kriging-based reliability analysis
- 2 method can be conducted based on this strategy.

12

4. Bayesian Updating with System Reliability Analysis Methods

- 4 To draw samples based on the posterior distribution with minimum number of evaluations of the likelihood
- 5 function L(x), an innovative approach is proposed here that leverages merits of both simple rejection
- 6 sampling method and adaptive Kriging-based reliability analysis techniques. Inspired by the work in [4],
- 7 which transforms the Bayesian updating problem into an equivalent reliability analysis problem with an
- 8 auxiliary random variable, the proposed method transforms the problem into a series-system reliability
- 9 analysis with multiple limit state functions. The main advantage of this strategy is that the acceptance rate
- in each decomposed limit state function is significantly improved, which facilitates the implementation of
- adaptive Kriging-based Reliability analysis in conjunction with simple rejection sampling.

4.1 SRS with Multiple Auxiliary Random Variables (SRS-MARV)

- 13 As explained in section 3, the direct implementation of Kriging-based reliability analysis for the limit state
- function in Eq. (12) can lead to high computational burdens when the number of observations increases, as
- acceptance rate will be extremely small for such cases. To overcome this limitation, a method is proposed
- that decomposes Eq. (12) into multiple limit state functions with high acceptance rate. First, note that the
- 17 likelihood function L(x) in Eq. (5) can be decomposed into multiple functions $W_i(x)$ as follows:

$$L(\mathbf{x}) = \prod_{i=1}^{n_l} W_i(\mathbf{x})$$
 (22)

- where n_l is the number of decomposed likelihood functions. Here, n_l is recommended to be equal to the
- 20 number of observations m; however that is not necessary. Let $[p_1, p_2 \dots p_{n_l}]$ be a set of mutually
- 21 independent standard uniform random variables in [0,1]. Then a domain can be defined according to the
- 22 augmented outcome space $[x, p_1, p_2 ... p_{n_l}]$:

23
$$\Omega_{acc}^{i} = [p_{i} \le c_{i} W_{i}(x)], i = 1, ... n_{l}$$
 (23)

- where Ω^i_{acc} , $i=1,2,...,n_l$ are the subsets of the accepted domain $\Omega_{acc}=\left[\Omega^1_{acc}\cap\Omega^2_{acc}...\cap\Omega^n_{acc}\right]$ and
- 2 $c_i = \frac{1}{max(W_i(x))}$, $i = 1, ... n_l$ are the corresponding constants to ensure $c_i W_i(x)$ is less than 1. Samples
- 3 $[x, p_1, p_2 ... p_{n_l}]$ generated from prior distribution f(x) in the accepted domain follow the posterior
- distribution f'(x). Hence, the acceptance region, Ω_{acc} , can be further expanded as:

$$\Omega_{acc} = \left[\Omega_{acc}^{1} \cap \Omega_{acc}^{2} \dots \cap \Omega_{acc}^{n_{l}} \right] = [Max\{p_{i} - c_{i}W_{i}(x)\} \leq 0], \qquad i = 1, \dots n_{l}$$
 (24)

6 Subsequently, the posterior distribution f'(x) can be determined as:

$$f'(\mathbf{x}) = \frac{\int_{p_{n_l} \in \Omega_{acc}^{n_l}} \cdots \int_{p_1 \in \Omega_{acc}^{1}} f(\mathbf{x}) dp_1 \cdots dp_{n_l}}{\int_{[\mathbf{x}, p_{n_l}] \in \Omega_{acc}^{n_l}} \cdots \int_{[\mathbf{x}, p_1] \in \Omega_{acc}^{1}} f(\mathbf{x}) dp_1 \cdots dp_{n_l} d\mathbf{x}}$$

$$= \frac{\int_0^1 I_{n_l}^{acc} ([\mathbf{x}, p_{n_l}] \in \Omega_{acc}^{n_l}) \cdots \left[\int_0^1 I_1^{acc} ([\mathbf{x}, p_1] \in \Omega_{acc}^{1}) f(\mathbf{x}) dp_1\right] \cdots dp_{n_l}}{\int_{\mathbf{x}} \int_0^1 I_{n_l}^{acc} ([\mathbf{x}, p_{n_l}] \in \Omega_{acc}^{n_l}) \cdots \left[\int_0^1 I_1^{acc} ([\mathbf{x}, p_1] \in \Omega_{acc}^{1}) f(\mathbf{x}) dp_1\right] \cdots dp_{n_l} d\mathbf{x}}$$

$$(25)$$

7 The numerator of Eq. (25) can be further expanded into the equation below:

$$\int_{p_{n_{l}} \in \Omega_{acc}^{n_{l}}} \cdots \int_{p_{1} \in \Omega_{acc}^{1}} f(\mathbf{x}) dp_{1} \cdots dp_{n_{l}}$$

$$= \int_{0}^{c_{n_{l}} L_{n_{l}}(\mathbf{x})} \cdots \int_{0}^{c_{1} L_{1}(\mathbf{x})} f(\mathbf{x}) dp_{1} \cdots dp_{n_{l}}$$

$$= \int_{0}^{c_{n_{l}} L_{n_{l}}(\mathbf{x})} \cdots \int_{0}^{c_{2} L_{2}(\mathbf{x})} c_{1} L_{1}(\mathbf{x}) f(\mathbf{x}) dp_{2} \cdots dp_{n_{l}}$$

$$= f(\mathbf{x}) \prod_{i=1}^{n_{l}} (c_{i} W_{i}(\mathbf{x})) = L(\mathbf{x}) \cdot f(\mathbf{x}) \cdot \prod_{i=1}^{n_{l}} c_{i}$$
(26)

8 Moreover, the denominator of Eq. (25) can be expanded to the following expression:

$$\int_{[x,p_{n_{l}}]\in\Omega_{acc}^{n_{l}}} \cdots \int_{[x,p_{n_{l}}]\in\Omega_{acc}^{n_{l}}} f(\mathbf{x}) dp_{1} \cdots dp_{n_{l}}$$

$$= \int_{X} \int_{0}^{1} I_{n_{l}}^{acc} ([\mathbf{x},p_{n_{l}}]\in\Omega_{acc}^{n_{l}}) \cdots \left[\int_{0}^{1} I_{1}^{acc} ([\mathbf{x},p_{1}]\in\Omega_{acc}^{1}) f(\mathbf{x}) dp_{1}\right] \cdots dp_{n_{l}} d\mathbf{x}$$

$$= \int_{X} \int_{0}^{1} I_{n_{l}}^{acc} (p_{n_{l}} \leq c_{n_{l}} W_{n_{l}}(\mathbf{x})) \cdots \left[\int_{0}^{1} I_{1}^{acc} (p_{1} \leq c_{1} L_{1}(\mathbf{x})) f(\mathbf{x}) dp_{1}\right] \cdots dp_{n_{l}} d\mathbf{x}$$

$$= \int_{X} f(\mathbf{x}) \prod_{i=1}^{n_{l}} (c_{i} W_{i}(\mathbf{x})) d\mathbf{x} = \left(\prod_{i=1}^{n_{l}} c_{i}\right) \cdot \int_{X} f(\mathbf{x}) \left(\prod_{i=1}^{n_{l}} W_{i}(\mathbf{x})\right) d\mathbf{x} = \left(\prod_{i=1}^{n_{l}} c_{i}\right) \cdot \int_{X} f(\mathbf{x}) L(\mathbf{x}) d\mathbf{x}$$

$$(27)$$

- 1 Different from SRS approach, SRS-MARV introduces multiple auxiliary random variables to decompose the
- 2 limit state in Eq. (12) into multiple limit state functions. Acceptance rates of these limit state functions are
- 3 significantly larger than those of SRS. The process for the implementation of SRS-MARV is summarized in
- 4 Algorithm 4.

Algorithm 4. Simple Rejection Sampling with Multiple Auxiliary Random Variables (SRS-MARV)

- 1. i = 1
- 2. Generate a sample x^i from f(x)
- 3. Generate multiple samples $\vec{p}^i = [p_1^i, p_2^i, ... p_m^i]$ from the standard uniform distribution [0.1]
- 4. If $[\mathbf{x}^i, \mathbf{p}^i] \in \Omega_{acc}$ by judging Eq. (24)
 - (a). Accept x^i
 - (b). i = i + 1
- 5. Stop if $i = N_s$, else go to step 2

6

7 4.2 Bayesian Updating using Adaptive Kriging (BUAK)

- 8 By integrating Kriging-based reliability analysis method and SRS-MARV, a new method called BUAK
- 9 (Bayesian Updating using Adaptive Kriging) is proposed for Bayesian updating. BUAK is a surrogate
- model-based Bayesian updating technique that can estimate the posterior distribution f'(x) with a small
- number of calls to the likelihood function L(x). This method is elaborated in Algorithm 5 and a flowchart
- that illustrates this method is also shown in Fig. 1. To check if the Kriging model is trained sufficiently, the
- 13 following stopping criterion Ψ in step 8 is proposed:

$$\Psi = \frac{\sum_{i=1}^{N_{acc}} \left\{ \Phi\left(-U(x)\right) \left(1 - \Phi\left(-U(x)\right)\right) \right\}}{N_{acc}} \le \Psi_{thr}$$
 (28)

- where N_{acc} is the number of accepted samples with the posterior distribution, $\Phi(\cdot)$ denotes the Cumulative
- Density Function (CDF) of the standard normal distribution and Ψ_{thr} is the stopping criterion threshold for
- 17 Kriging active learning. According to [34], the total number of wrong sign estimation follows a Poisson
- 18 Binomial distribution, thus, Ψ is an indicator of the expected variance of the total number of wrong
- 19 classified samples for accepted or failure points. It should be noted that the U function in Eq.(20) is an
- 20 appropriate model to identify the next best training points. However, if used as a stopping criterion in the

- form of max $max(U) \le U_{thr}$, it leads to a large number of unnecessary calls to the performance function
- 2 in Bayesian updating problems. The proposed model in Eq.(28) addresses this problem and yields accurate
- 3 Kriging model for Bayesian updating.

Algorithm 5. Bayesian Updating using Adaptive Kriging

- 1. Define the parameters:
 - (a). Number of candidate design samples n_d and training samples n_{tr}
 - (b). Number of decomposition of likelihood function L(x) as n_l
 - (c). Number of dimension of random variable X as n_X
 - (d). Constant c_i , $i = 1, ... n_l$
- 2. Using Latin Hypercube Sampling technique (*LHS*) to generate following samples :
 - (a). n_d candidate design samples x_d and p_d from f(x) and standard uniform distribution [0,1] where x_d is a $n_d \times n_X$ matrix and p_d is a $n_d \times n_l$ matrix with number of decomposition of likelihood function as column. Denote the set of candidate design samples set as D.
 - (b). n_{tr} candidate design samples x_{tr} and p_{tr} from prior distribution f(x) and standard uniform distribution [0,1]
 - (c). Define the training samples set $T = [\mathbf{x}_{tr}, \mathbf{p}_{tr}]$ and denote its subset as $T_1 = [\mathbf{x}_{tr}, p_{tr}^1]$, ... $T_{n_l} = [\mathbf{x}_{tr}, p_{tr}^{n_l}]$, where $p_{tr}^i, i = 1, ..., n_l$ is the i_{th} column vector in \mathbf{p}_{tr}
- 3. j = 1
- 4. Evaluate all the responses \mathbf{y}_{tr}^i , i=1,... n_l of $T_1=[\mathbf{x}_{tr},p_{tr}^1]$, ... $T_{n_l}=[\mathbf{x}_{tr},p_{tr}^{n_l}]$ corresponding to all the limit state functions h_i , i=1,... n_l , where \mathbf{y}_{tr}^i is a $n_{tr} \times 1$ matrix.
- 5. Construct the j_{th} Kriging models \hat{h}_i according to the training samples subset T_i .
- 6. Estimate the responses (e.g., mean μ_j and variance σ_j^2) of candidate design samples D based on j_{th} Kriging models \hat{h}_i .
- 7. Compute the value of U learning function for candidate design samples D using the Kriging model \hat{h}_i .
- 8. Check if $\Psi \leq \Psi_{thr}$ is satisfied or not:
 - (a). Satisfied. Go to step 9.
 - (b). Unsatisfied. Search for the next best training point $[x_{tr}^*, p_{tr}^*]$ in D, renew T and go back to Step 4.
- 9. Check if $j > n_l$ is satisfied or not:
 - (a). Satisfied. Go to step 10.
 - (b). Unsatisfied. Do j = j + 1 and go back to Step 4.
- 10. Implement SRS-MARV based on n_l surrogate Kriging model \hat{h}_i , $i=1,...n_l$ according to the Algorithm 4.

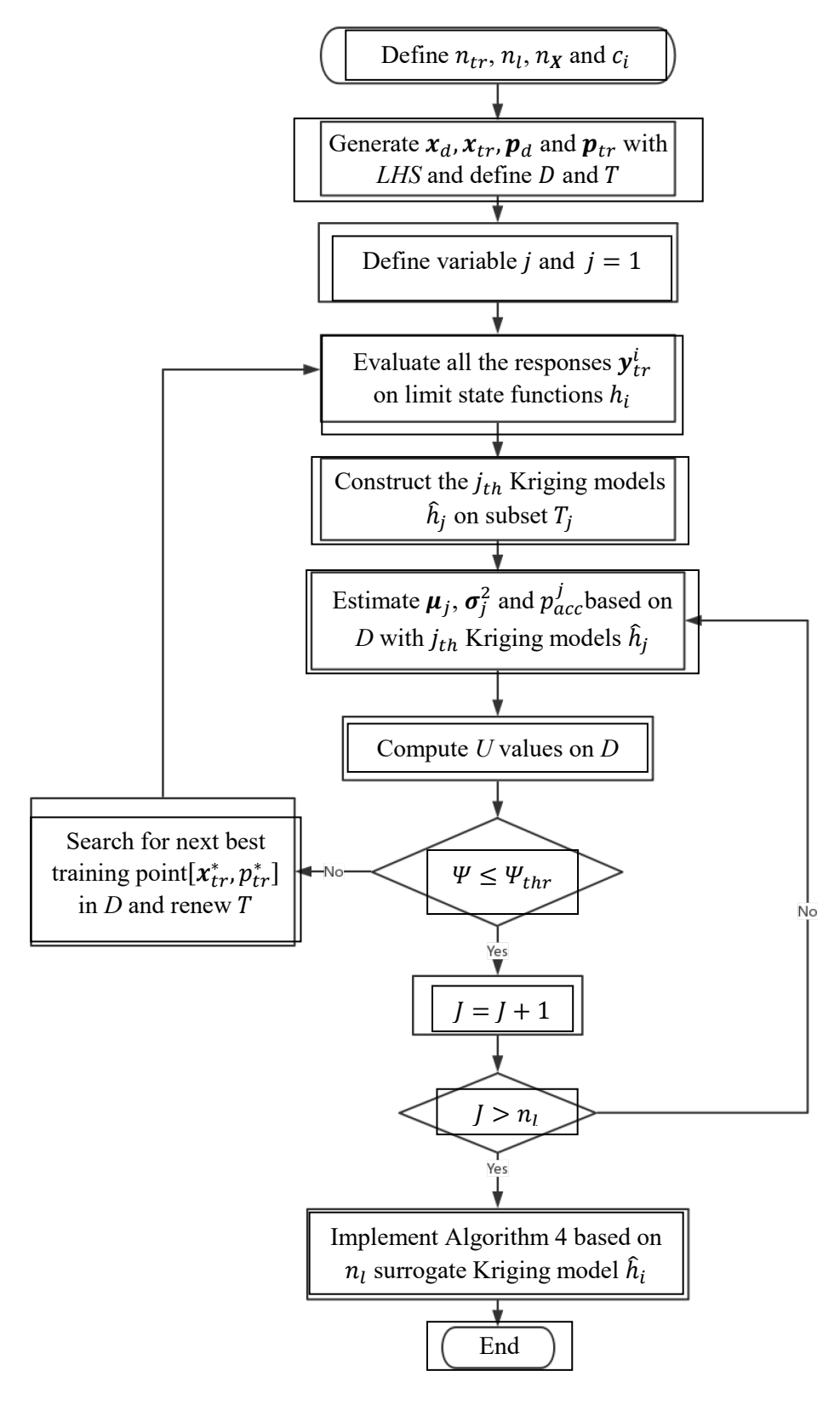


Fig 1. Flowchart of BUAK

5. Numerical Studies

1

- 2 In this section, three numerical examples are implemented to investigate the performance of the proposed
- 3 method *BUAK* compared to existing techniques.

4 5.1 Example 1: Illustrative purpose

- 5 The first example is implemented here to illustrate the general process of the proposed method *BUAK*. This
- 6 example has also been studied in [5]. The problem involves a one-dimensional random variable that follows
- 7 a standard normal prior distribution, denoted as $\varphi(x)$. The likelihood of this problem also follows a normal
- 8 distribution with mean $\mu_l = 3$ and standard deviation $\sigma_l = 0.3$. Thus the maximum value of this likelihood
- 9 is $L_{max} = \frac{1}{\sigma_l \sqrt{2\pi}} = 1.33$, which means $c = \frac{1}{max(L_{max})} = 0.752$. The limit state function according to Eq.
- 10 (12) can be represented as:

$$h(x,p) = p - c\phi(x|\mu_l, \sigma_l)$$
 (29)

- where p is an auxiliary random variable following the standard uniform distribution and $\phi(x|\mu_l,\sigma_l)$
- denotes the probability density function of a normal distribution parameterized by μ_l and σ_l . To reduce the
- nonlinearity of Eq. (29), the logarithmic formulation of the limit state function (i.e., Eq.(29)) can be used
- 15 as follows [5]:

$$g(x,p) = \ln(p) - \ln(c) - \ln(\phi(x|\mu_l, \sigma_l))$$
(30)

- In this one dimensional example, the acceptance rate, P_{acc} , is 4.63×10^{-3} , which allows implementation
- 18 of Monte Carlo simulations with BUS method as a benchmark with high accuracy. Thus, four methods
- including BUS + MCS, BUS + Subset Simulation (SS), BUAK + MCS and BUAK + SS are explored in this
- 20 example. For this problem, the number of initial training points and candidate design samples are selected
- as 12 and 10^5 , respectively. The performance of the considered methods is evaluated in terms of the number
- of calls to the likelihood function, N_{call} ; ratios between the true and estimated mean and standard deviation
- of the posterior distribution (i.e., $\hat{\mu}/\mu'$ and $\hat{\sigma}'/\sigma'$), and the confusion matrix.
- Results of the analyses are summarized in Table 1. With 10⁵ samples for Monte Carlo simulations, the
- mean and standard deviation of posterior distribution estimated through BUS + MCS can reach very high

accuracy with $\frac{\hat{\mu}'}{\mu'} = 0.9991$ and $\frac{\hat{\sigma}'}{\sigma'} = 1.0377$. However, it needs an extremely large number of calls to the 1 performance function (i.e., $N_{call} = 10^5$), which is not feasible in practice. The proposed surrogate model-2 based approach, BUAK + MCS, can dramatically reduce the number of calls to the performance function to 3 $N_{call}=26$, while offering a relatively high accuracy with $\frac{\hat{\mu}'}{\mu'}=1.0072$ and $\frac{\hat{\sigma}'}{\sigma'}=0.9492$. The reason for 4 5 high computational efficiency is that the proposed method only needs the calls to performance function to 6 explore and refine the limit state. Figure 2 shows the true limit state of Eq. (29) or (30) and the limit state estimated using BUAK with $N_{call} = 15$ and $N_{call} = 26$. According to Fig. 2, the estimated limit state 7 function $\hat{h}(x, p) = 0$ gradually refines as the number of training points x_{tr} increases. The accepted samples 8 and samples that are wrongly estimated from the prior distribution are illustrated in Fig. 3. Totally, the label 9 of 17 points out of 10⁵ points is wrongly estimated (i.e., points that should be accepted but are rejected, 10 and points that should be rejected but are accepted). To further investigate the performance of the proposed 11 surrogate-based approach, the confusion matrix of rejected and accepted samples of BUAK + MCS is 12 13 presented in Table 2. According to this confusion matrix, there are totally 5 samples out of 451 that should 14 be accepted but rejected through the proposed approach. Moreover, the 'precision' (P) and 'recall' (R) of this confusion matrix are found as $P = \frac{99525}{99525+5} = 0.9998$ and $R = \frac{99525}{99525+24} = 0.9998$. Thus, the 15 probabilities of failure for the true and estimated limit state functions are 0.0045 and 0.0047, respectively, 16 which indicates an error of $\epsilon = 0.0444$. These values indicate that the proposed method, BUAK, is 17 computationally accurate. The ratios of the means and standard deviations of the estimated to true posterior 18 distributions using BUS + SS are $\frac{\hat{\mu}'}{\mu'} = 1.0428$ and $\frac{\hat{\sigma}'}{\sigma'} = 0.9279$, respectively, with $N_{call} = 3749$. The 19 parameters of the posterior distribution estimated through BUAK + SS are shown to be even more accurate 20 than BUS + SS with $\frac{\hat{\mu}'}{\mu'} = 1.0375$ and $\frac{\hat{\sigma}'}{\sigma'} = 0.9441$, with $N_{call} = 26$. Figure 4 shows accepted samples in 21 22 different stages of subset simulation in BUAK + SS. The estimation error of BUAK + SS can be explained by the fact that the estimated limit state does not completely match the true limit state. As more training 23

- 1 points are added in training the surrogate model, it is expected that the accuracy of the parameters of the
- 2 posterior distribution estimated using BUAK + MCS and BUAK + SS increases.

5

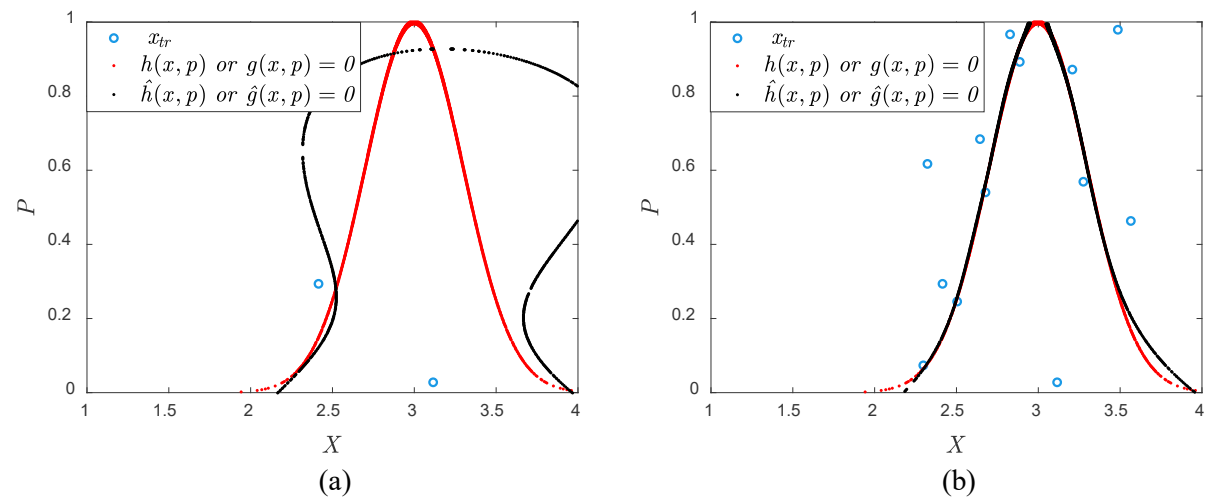


Fig. 2. The true limit state function h(x, p) = 0 and that estimated using BUAK $\hat{h}(x, p) = 0$ with (a) $N_{call} = 15$ and (b) $N_{call} = 26$.

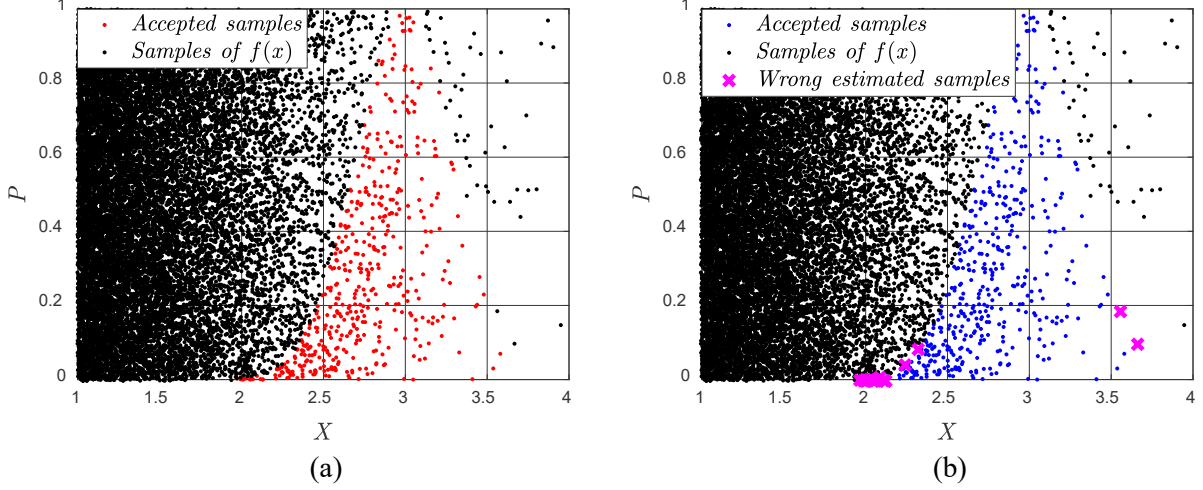


Fig. 3. Illustration of accepted samples through (a) BUS + MCS and (b) BUAK + MCS.

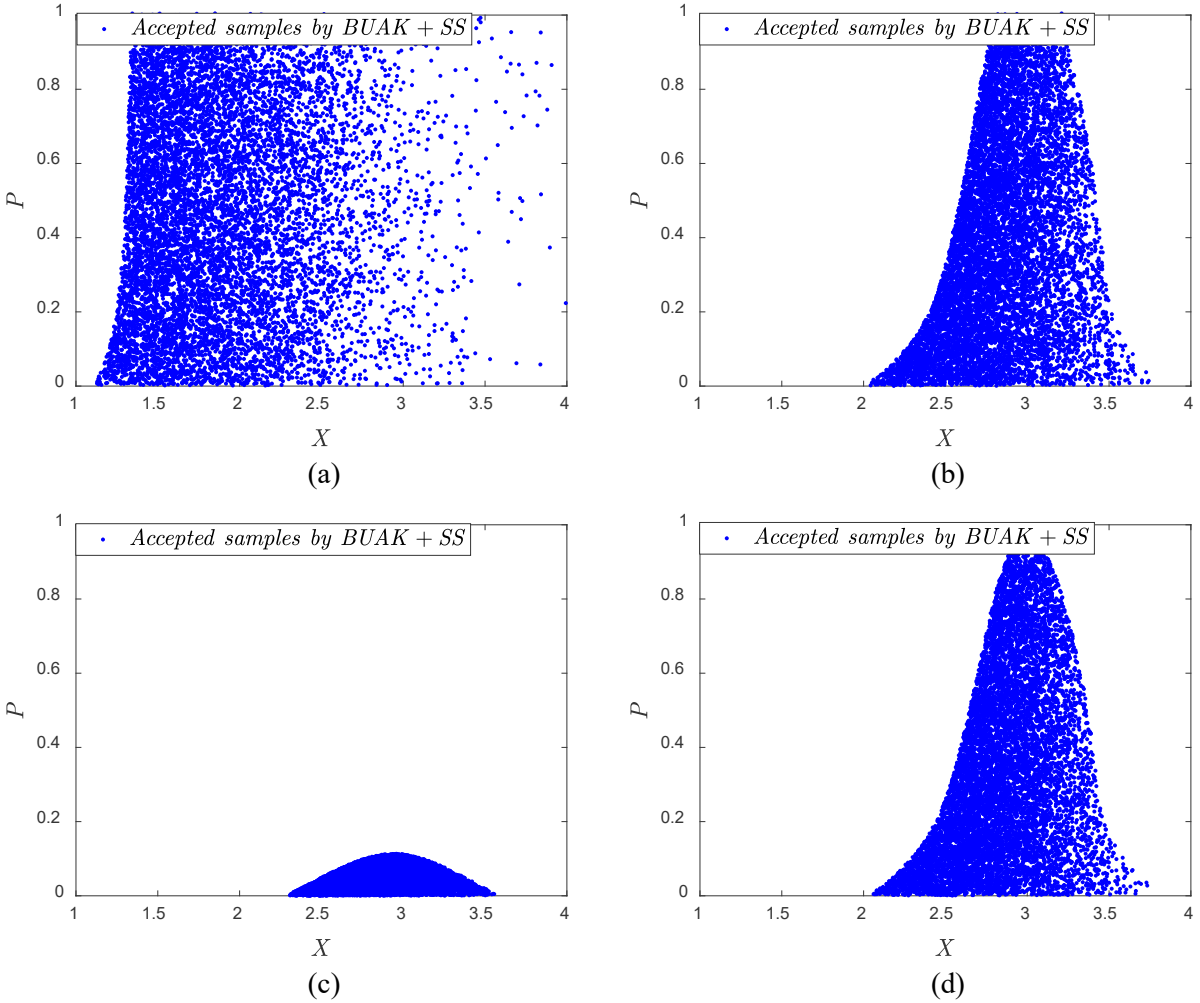


Fig. 4. Illustration of BUAK + SS with accepted samples in (a) the first subset, (b) the second subset, (c) the third subset, and (d) the last subset.

Table 1. Bayesian Updating results for BUS + MCS, BUAK + MCS, BUS + SS, and BUAK + SS. The initial number of training points for BUAK is 12, while the number of candidate design samples is 10^5 . $\hat{\mu}'/\mu'$ and $\hat{\sigma}'/\sigma'$ denote the true/estimated mean and true/estimated standard deviation of the posterior distribution, respectively.

Methodology	N_{call}	μ'	σ'	$\hat{\mu}'$	$\hat{\sigma}'$	$\hat{\mu}'/\mu'$	$\hat{\sigma}'/\sigma'$
BUS + MCS	10^{5}			2.7474	0.2978	0.9991	1.0377
BUAK + MCS	12 + 14	2.75	0.287	2.7697	0.2724	1.0072	0.9492
BUS + SS	3749	2.73	0.287	2.8677	0.2663	1.0428	0.9279
BUAK + SS	12 + 14			2.8530	0.2709	1.0375	0.9441

Table 2. Confusion matrix for the results of BUAK + MCS approach.

Actual	Predicted Class			
Class	Rejected	Accepted		
Rejected	99525	24		
Accepted	5	446		

Note that running a single simulation with a prechosen number of samples may not provide a comprehensive assessment of the performance of stochastic estimators. This is due to the fact that randomness exists in the selection of initial training and candidate design samples. To examine such effects, the expected performance and the variation in the performance of Bayesian updating methods are investigated here. 100 simulations are used to evaluate these measures and the results are summarized in Table 3. Four methods including BUS + MCS, BUAK + MCS, BUS + SS and BUAK + SS are examined by computing the expected number of calls to the limit state function $E(N_{call})$, expected value of the estimated mean $E(\hat{\mu}'/\mu')$ and standard deviation $E(\hat{\sigma}'/\sigma')$ and their corresponding coefficients of variation(C.O.V). Results indicate that BUS + MCS is the most accurate method with $E(\hat{\mu}'/\mu') = 1.001$ and $E(\hat{\sigma}'/\sigma') = 1.006$. However, BUAK + MCS achieves the high accuracy of $E(\hat{\mu}'/\mu') = 1.005$ with $E(N_{call}) = 31.02$, as compared to $E(N_{call}) = 10^5$ for BUS + MCS.

Table 3. The performance of Bayesian Updating with 100 simulations for example 1.

Methodology	$E(N_{call})$	$C.O.V$ (N_{call})	$E(\hat{\mu}'/\mu')$	C.O.V (µ̂'/µ')	$E(\hat{\sigma}'/\sigma')$	$C.O.V$ $(\hat{\sigma}'/\sigma')$
BUS + MCS	10^{5}	-	1.001	0.004	1.006	0.022
BUAK + MCS	31.02	0.596	1.005	0.007	0.960	0.043
BUS + SS	3812.5	0.051	1.034	0.001	0.941	0.017
BUAK + SS	31.02	0.596	1.046	0.003	0.931	0.035

5.2 Example 2: Unimodal distribution

The second example has a posterior distribution with *n*-dimensional random variables [3], [37]. First, the prior distribution of the random variables can be represented as the multiplication of *n* mutually independent standard normal distributions $f(x) = \prod_{i=1}^{n} \varphi(x_i)$. The likelihood function L(x) can be represented as:

$$L(x) = \prod_{i=1}^{n} \frac{1}{\sigma_i} \phi(x_i | \mu_i, \sigma_i)$$
(31)

20 where σ_l is set as 0.2 and μ_l can be computed as follows:

$$\mu_l = \sqrt{-2(1+\sigma_l^2) \cdot ln \left[c_E^{1/n} \cdot \sqrt{2\pi \cdot \sqrt{1+\sigma_l^2}} \right]}$$
(32)

- where c_E is the model evidence. Two cases including (a) n=2 and $c_E=10^{-4}$ and (b) n=10 and $c_E=10^{-4}$
- 3 10^{-5} are investigated in this example. According to Eq. (12), the limit state function of the SRS method
- 4 can be written as:

$$h(\mathbf{x}, p) = p - c \prod_{l=1}^{n} \frac{1}{\sigma_l} \phi(x_i | \mu_l, \sigma_l)$$
(33)

- For the first case (i.e., n=2 and $c_E=10^{-4}$), the acceptance rate, P_{acc} , is equal to 2.451×10^{-5} , which
- 7 indicates that a large number of candidate design samples are required to capture the limit state in Eq. (33)
- 8 and subsequently estimate f'(x) through BUAK+SRS. The large number of candidate design samples
- 9 makes the BUAK + SRS computationally inefficient. To increase P_{acc} for Eq. (33), SRS-MARV should be
- adopted here as explained in Eq. (22):

11
$$L(\mathbf{x}) = \prod_{l=1}^{n} \frac{1}{\sigma_l} \phi(x_i | \mu_l, \sigma_l) = \prod_{l=1}^{n_l} W_i(x_l)$$
 (34)

- where n_l is the number of decompositions of the likelihood function and $n_l = n$, which means that the
- decomposed likelihood function can be presented as follows:

14
$$W_1(x_1) = W_2(x_2) = \cdots W_i(x_i) = \frac{1}{\sigma_i} \phi(x_i | \mu_i, \sigma_i) \text{ and } c_i = \frac{1}{\max(W_i(x_i))}$$
 (35)

- Since all the formulations of $W_i(x_i)$ have the same format, only one surrogate model for the limit state
- 16 function is required according to Eq. (12),

17
$$h(x_i, p_i) = p_i - c_i W_i(x_i)$$
 (36)

- where p_i , i = 1, ..., n are the n auxiliary random variables that follow uniform distribution. The acceptance
- 19 rate involving the limit state function in Eq. (36) is relatively very high, which indicates that the required
- number of candidate design samples and required training samples can be small when using BUAK + SRS-

- 1 MARV. Moreover, Eq. (36) can be further expanded to reduce the nonlinearity by taking the logarithmic
- 2 form:

$$g(x_i, p_i) = \ln(p_i) - \ln(c_i) - \ln(W_i(x_i))$$
(37)

For the first case where n=2, $P_{acc}=2.451\times 10^{-5}$, $\mu'=2.659$ and $\sigma'=0.1961$. Five methods 4 including BUS+MCS+SRS, BUS+MCS+SRS-MARV, BUS+SS+SRS-MARV, BUAK+MCS+SRS-MARV, 5 6 and BUAK+SS+SRS-MARV are investigated to explore the performance of the proposed method. Results 7 of these methods are summarized in Table 4. For the active learning in BUAK, 12 initial training samples and 10⁵ candidate design samples are prepared. The accuracy of the considered methods is evaluated in 8 9 terms of the estimated mean and standard deviation of the posterior distribution (i.e., $\hat{\mu}'$ and $\hat{\sigma}'$). Figure 5 shows the true limit state, $h(x_i, p_i)$, and the estimated limit state, $\hat{h}(x_i, p_i)$, through Kriging surrogate model 10 at different stages of training including $N_{call} = 20$ and 31. The probabilities of failure for the true and 11 estimated limit state functions (e.g., $h(x_i, p_i)$ and $\hat{h}(x_i, p_i)$) are estimated as 0.00509 and 0.00503, which 12 indicates the corresponding error is estimated as $\epsilon = 0.012$. Among all of these approaches, $\hat{\mu}'$ and $\hat{\sigma}'$ 13 estimated through BUS+MCS+SRS and BUS+MCS+SRS-MARV are the most accurate with $\frac{\hat{\mu}'}{u'} = 1.0008$ 14 and $\frac{\hat{\sigma}'}{\sigma'} = 0.9870$ for BUS+MCS+SRS, and $\frac{\hat{\mu}'}{\mu'} = 0.9977$ and $\frac{\hat{\sigma}'}{\sigma'} = 1.0125$ for BUS+MCS+SRS-MARV. 15 However, these methods require a significantly large number of calls to the performance function with 16 $N_{call} = 2 \times 10^7$, which is intractable for sophisticated models. The BUS algorithm with subset simulation 17 can significantly reduce the number of evaluations of the performance function with $N_{call} = 28384$ when 18 $N_{in} = 5000$ for each subset. The BUS+SS approach can still achieve high accuracy in estimating the 19 posterior distribution f'(x) with $\frac{\hat{\mu}'}{\mu'} = 1.0066$ and $\frac{\hat{\sigma}'}{\sigma'} = 1.051$. The proposed method *BUAK+MCS+SRS*-20 MARV is shown to be computationally very efficient and accurate. With only 31 evaluations of the 21 performance function, the ratios of the estimated to true means and standard deviations are $\frac{\hat{\mu}'}{\mu'} = 1.0031$ 22 and $\frac{\hat{\sigma}'}{\sigma'} = 0.9446$. Figure 6 shows samples from the posterior distribution estimated through 23

1 BUS+MCS+SRS, BUS+MCS+SRS-MARV, BUS+SS+SRS-MARV, and BUAK+MCS+SRS-MARV. The main deviation of BUAK+MCS+SRS-MARV (Fig. 6(d)) from BUS+MCS+SRS-MARV (Fig. 6(b)), is that 2 BUAK+MCS+SRS-MARV rejects some 'outlier' points, which makes $\hat{\sigma}'$ smaller. These points are referred 3 4 to the points that are in the failure domain with extremely low probability density in the equivalent 5 reliability analysis problems. Therefore, these 'outlier' points can only be precisely captured if the Kriging-6 based reliability method is set with extremely tight stopping criterion (i.e., $\Psi_{thr} \rightarrow 0$). For the case where n=10, $\mu'=0.6542$ and $\sigma'=0.1961$, P_{acc} is extremely small and difficult to estimate. Thus, two 7 8 methods including BUS+SS and BUAK+SS are investigated for this case. Since the example 2 is based on 9 the SRS-MARV strategy, for the purpose of consistency, the proposed method is compared with BUS+SS+SRS-MARV and not BUS+SS+SRS. Although the original BUS+SS-SRS is not investigated here, 10 11 it is expected to outperform BUS+SS+SRS-MARV. This is related to constants c_i , $i=1,...n_l$, which are chosen as $\frac{1}{max(L_i(x))}$ for the component reliability problems in the system formulation for the SRS-MSRV 12 13 strategy. This choice leads to a much smaller acceptance probability for the overall parallel system as compared to the case where the original BUS formulation is used where c is chosen close to $\frac{1}{max(L(x))}$. In 14 table 5, $\hat{\mu}'/\mu'$ and $\hat{\sigma}'/\sigma'$ denote the true/estimated mean and standard deviation of the posterior distribution 15 16 based on one of the components of vector x. For this case, the number of samples in each level of SS is selected as 10⁴. For the state-of-the-art approach BUS+SS where c is identified adaptively, interested readers 17 are referred to [5]. Results indicate that the accuracy of estimated f'(x) improves as the stopping criterion 18 becomes tight with $\Psi_{thr} = 1 \times 10^{-5}$. These results indicate that the proposed BUAK algorithm is very 19 20 capable for Bayesian updating, especially for cases involving sophisticated models.

Table 4. Bayesian Updating results of BUS + SS and BUAK + SS for example 2 (n = 2). $\hat{\mu}'/\mu'$ and $\hat{\sigma}'/\sigma'$ denote the true/estimated means and standard deviations of the posterior distribution based on one of the components of vector \mathbf{x} . $\Psi_{thr} = 1 \times 10^{-3}$ is set in this case.

21

22

Methodology	Sampling method	N_{call}	μ́′	$\hat{\sigma}'$	$\hat{\mu}'/\mu'$	$\hat{\sigma}'/\sigma'$
BUS + MCS	SRS	2×10^{7}	2.6612	0.1936	1.0008	0.9870
BUS + MCS	SRS-MARV	2×10^{7}	2.6529	0.1986	0.9977	1.0125
BUS + SS	SRS-MARV	28384	2.6765	0.2061	1.0066	1.051
BUAK + MCS	SRS-MARV	12 + 19	2.6674	0.1853	1.0032	0.9446
BUAK + SS	SRS-MARV	12 + 19	2.7310	0.2068	1.0271	1.0544

1 **Table** 5. Bayesian Updating results of BUS + SS and BUAK + SS for example 2 (n = 10).

	0				\	
Methodology	Sampling method	N_{call}	$\hat{\mu}'$	$\hat{\sigma}'$	$\hat{\mu}'/\mu'$	$\hat{\sigma}'/\sigma'$
	memou					
BUS + SS	SRS-MARV	64886	0.6778	0.1811	1.036	0.9236
$BUAK + SS$ $(\Psi_{thr} = 1 \times 10^{-3})$	SRS-MARV	12 + 25	0.5902	0.1654	0.9021	0.8433
$BUAK + SS$ $(\Psi_{thr} = 1 \times 10^{-4})$	SRS-MARV	12 + 73	0.6144	0.1730	0.9392	0.8821
$BUAK + SS$ $(\Psi_{thr} = 1 \times 10^{-5})$	SRS-MARV	12 + 91	0.6222	0.1751	0.9511	0.8961

2

4

5

6

8

9

10

11

3 Similar to example 1, the expected performance the variation in the performance of Bayesian algorithms is investigated for example 2. The average performance based on 100 simulations is summarized in Table 6. Again, four methods including BUS + MCS, BUAK + MCS, BUS + SS and BUAK + SS are examined by computing the expected number of calls to the limit state function $E(N_{call})$, expected value of the estimated mean $E(\hat{\mu}'/\mu')$ and standard deviation $E(\hat{\sigma}'/\sigma')$ and their corresponding coefficients of variation (C.O.V). 7 An interesting observation is that the application of surrogate model in Bayesian updating can increase the variance of the estimated results. This observation is due to fact that the shape of the true limit state can not be perfectly captured by the surrogate model. However, despite this limitation, the results in Table 6

12

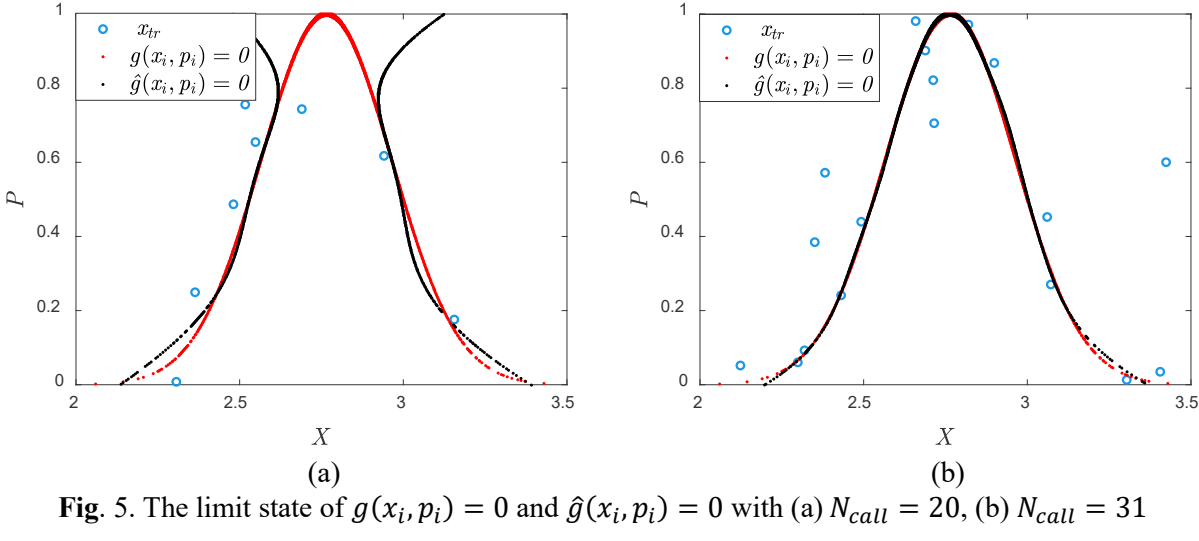
13

14

Table 6. The performance of Bayesian Updating with 100 simulations for example 2(Based on the SRS-MARV strategy).

showcase the computational efficiency of the proposed BUAK algorithm.

Methodology	$E(N_{call})$	$C.O.V$ (N_{call})	$E(\hat{\mu}'/\mu')$	C.O.V (μ̂'/μ')	$E(\hat{\sigma}'/\sigma')$	$C.O.V \ (\hat{\sigma}'/\sigma')$
BUS + MCS	2×10^{7}	-	0.999	0.001	0.998	0.010
BUAK + MCS	36.24	0.596	1.006	0.008	0.952	0.027
BUS + SS	26148	0.047	1.008	0.006	0.956	0.035
BUAK + SS	36.24	0.596	1.023	0.015	0.943	0.042



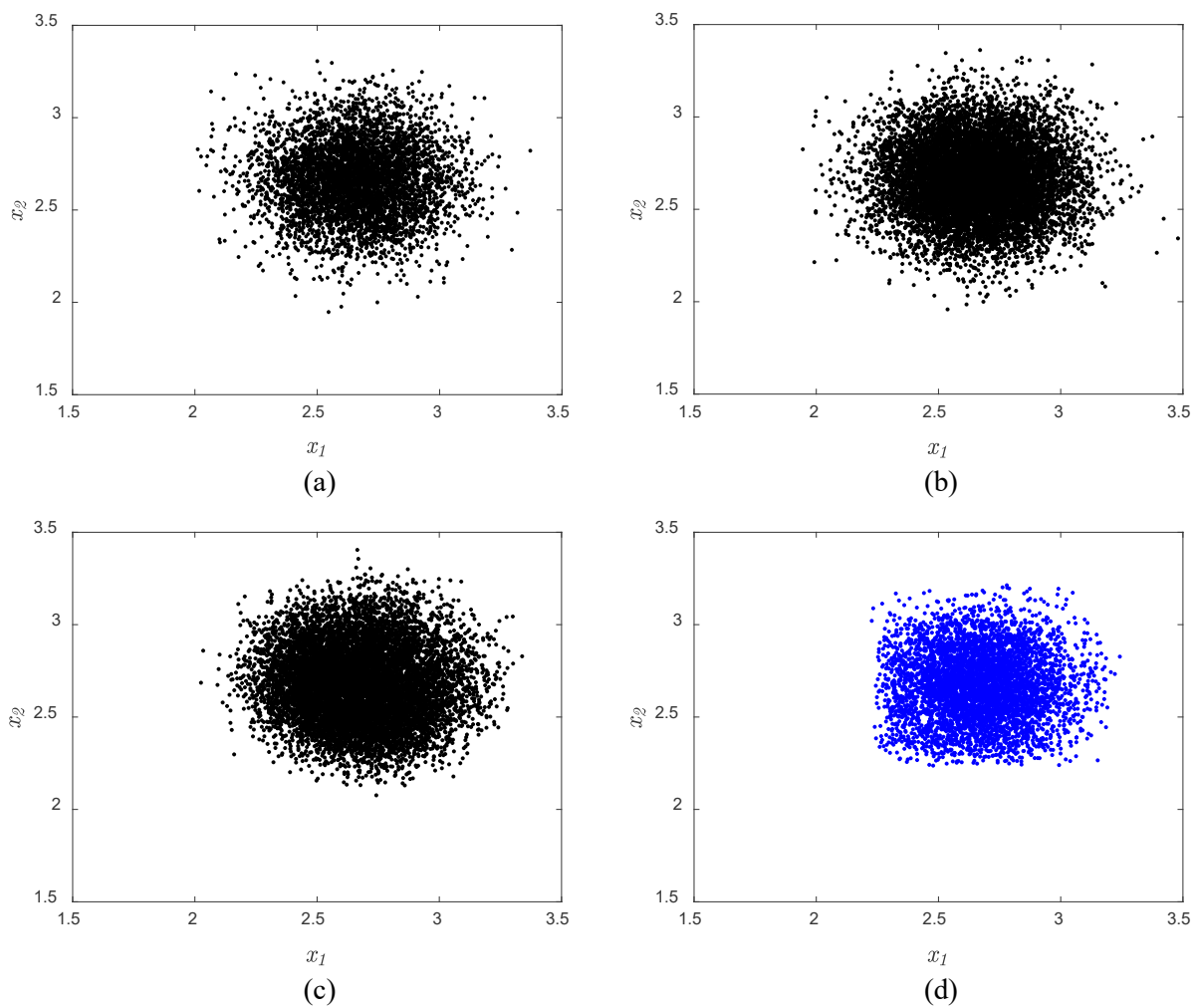


Fig. 6. f'(x) estimated through (a) BUS+MCS+SRS, (b) BUS+MCS+SRS-MARV, (c) BUS+SS+SRS-MARV, and (d) BUAK+MCS+SRS-MARV.

5.3 Example 3: Two degrees-of-freedom structure

2 The third example involving a two-degrees-of-freedom (two-DOF) system was originally developed in [1] and then investigated in [3]–[5] to assess the performance of BUS. The goal of this case study is to estimate 3 4 the posterior distribution of inter-story stiffnesses based on measurements of eigen-frequencies of the 5 structure. The configuration of this structure is shown in Fig. 7. The masses of the two stories are set as $m_1=16.531\cdot 10^3~kg$ and $m_2=16.13.1\cdot 10^3~kg$. The inter-story stiffnesses are modeled as $K_1=X_1k_n$ 6 and $K_2 = X_2 k_n$, where K_1 and K_2 are the stiffness values of the first and second stories, respectively, $k_n =$ 7 $29.7 \cdot 10^6 \, N/m$ is the nominal value, and X_1 and X_2 are correction factors to be updated. In this example, 8 9 damping is not considered. As stated before, the distribution of $X = [X_1, X_2]$ is updated according to the observations of the first two eigen-frequencies f_1 and f_2 . Referring to the work in [1], [4], the likelihood 10 11 function for this problem can be presented as:

12
$$L(x) \propto \exp\left[-\frac{J(x)}{2\sigma_{\varepsilon}^2}\right] \tag{43}$$

13 where

1

14
$$J(x) = \sum_{j=1}^{2} \lambda_j^2 \left[\frac{f_j^2(x)}{\tilde{f}_j^2} - 1 \right]^2$$
 (44)

is a measure-of-fit function. $f_j^2(x)$ is the *j*th eigen-frequency estimated from the structural model with random factors x, and \tilde{f}_j^2 is the measurement of the *j*th eigen-frequency. $\lambda_1 = \lambda_2 = 1$ are the means and $\sigma_{\varepsilon} = \frac{1}{16}$ is the standard deviation of the prediction error. In this example, two measurements of eigenfrequencies are available: $\tilde{f}_1 = 3.13$ Hz and $\tilde{f}_2 = 9.83$ Hz. The prior distribution of X_1 and X_2 are uncorrelated lognormal distributions with modes 1.3 and 0.8 and standard deviations $\sigma_{X_1} = \sigma_{X_2} = 1$.

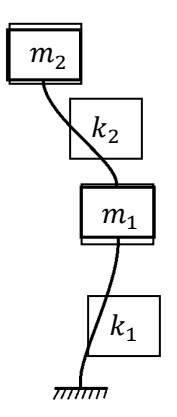


Fig. 7. Two-DOF shear building model.

14

15

16

17

18

19

According to the instructions of BUS algorithm, the original limit state function can be represented as:

$$h(x,p) = p - c \cdot \exp\left[-\frac{J(x)}{2\sigma_{\varepsilon}^2}\right]$$
 (45)

- 6 To increase the acceptance rate in Eq. (45) for the purpose of constructing the Kriging model, the likelihood
- 7 function can be decomposed into 2 likelihood functions:

$$W_i(\mathbf{x}) = \exp\left[-\frac{\lambda_i^2 \left[\frac{f_i^2(\mathbf{x})}{\tilde{f}_i^2} - 1\right]}{2\sigma_{\varepsilon}^2}\right], i = 1, 2$$
(46)

9 The two corresponding limit state functions, denoted as h_i , i = 1,2, can be subsequently represented as:

$$h_i(p_i, x) = p_i - c_i W_i(x_i), i = 1, 2$$
(47)

- where p_i , i = 1,2 are the two auxiliary random variables and c_i , i = 1,2 are the constants satisfying Eq. (24).
- 12 In this case, $c_1 = c_2 = 1$. The logarithmic form of Eq. (47) is:

13
$$g_i(x, p_i) = \ln(p_i) - \ln(c_i) - \ln(W_i(x)), i = 1, 2$$
 (48)

The acceptance rate of the undecomposed limit state function in Eq. (45) is about 0.0016, which indicates to the feasibility of integrating Monte Carlo simulations with BUS and BUAK algorithms as the benchmarks. Four methods are considered here including BUS+MCS, BUS+SS, BUAK+MCS, and BUAK+SS. The performance of these methods is evaluated in terms of the number of calls to the performance function N_{call} , and mean and standard deviation of the posterior distribution estimated in the left and right clusters (i.e., $\hat{\mu}'(L)$, $\hat{\mu}'(R)$, $\hat{\sigma}'(L)$ and $\hat{\sigma}'(R)$, L denotes $X_1 < 1$ and R denotes $X_1 > 1$).

1 Simulation results of these methods are summarized in Table 7. Figure 9 showcases the samples following posterior distribution using BUS+MCS through SRS and SRS-MARV strategies. According to these results 2 and those in Table 8, f'(x) estimated through BUS+MCS+SRS and BUS+MCS+SRS-MARV are very close. 3 Figure 9 offers a comparison between results generated using BUS+MCS+SRS-MARV and 4 5 BUAK+MCS+SRS-MARV. The manga cross points in Fig. 9 (b) are the wrongly accepted samples estimated 6 from the surrogate models, $\hat{g}_i(x, p_i)$, i = 1, 2, using the BUAK method compared with the true limit state 7 functions $g_i(x, p_i)$, i = 1, 2. The performance of this classification task is summarized in the confusion matrix in Table 8. Out of 2×10^5 candidate design samples, 321 samples should be accepted. The 8 'precision' (P) and 'recall'(R) of this confusion matrix are $P = \frac{199656}{199656+15} = 0.999$ and $R = \frac{199656}{199656+23} = 0.999$ 9 10 0.999, which indicate the very high accuracy of the involved classification. Thus, the probabilities of failure for the true and estimated limit state functions are 1.61×10^{-5} and 1.65×10^{-5} and the corresponding 11 error is calculated as $\epsilon = \frac{1.65 \times 10^{-5} - 1.61 \times 10^{-5}}{1.61 \times 10^{-5}} = 0.0248$, which is very small. The mean and standard 12 deviation of f'(x) estimated through BUAK+MCS+SRS-MARV are close to those estimated through 13 BUS + MCS + SRS - MARV with $\Delta_{\widehat{\mu}'(L)} = 0.4997 - 0.4996 = 0.0001$, $\Delta_{\widehat{\mu}'(R)} = 1.8093 - 1.8146 = 0.0001$ 14 $-0.0053,\,\Delta_{\widehat{\sigma}'(L)} = 0.0417 - 0.0406 = 0.0011 \text{ and } \Delta_{\widehat{\sigma}'(R)} = 0.1527 - 0.1544 = -0.0017. \text{ Results of } 0.0017 + 0.0018 = 0.0011$ 15 BUS+SS+SRS-MARV and BUAK+SS+SRS-MARV are shown in Fig. (10) and (11), respectively, which 16 17 demonstrate that the process of accepting the samples with posterior distribution is very close to that via 18 the true limit state. Results from Table 7 show that parameters of f'(x) estimated using BUAK+SS+SRS-MARV are close to the approach of BUS+SS+SRS-MARV with $\Delta_{\widehat{\mu}'(L)} = 0.5032 - 0.5038 = -0.0006$, 19 20 0.1476 = -0.0124. 21 22 For this example, BUS+SS needs 3758 calls to the performance function with 1000 samples searching 23 in each subsets. The proposed method BUAK is computationally very efficient as it requires only 250 24 training samples to achieve high accuracy. These training points include 12 initial training sample, 175

samples for training the first Kriging surrogate model (i.e., $\hat{g}_1(x, p_1)$) and 63 samples for training the second Kriging surrogate model (i.e., $\hat{g}_2(x, p_2)$). In the first loop for constructing \hat{h}_1 , the total number of evaluations to the performance function is 12 (initial training) + 175 (for \hat{h}_1). These 187 points can also be used in the construction of \hat{h}_2 . It should be noted that the 175 training points used for \hat{h}_1 are not strategically selected for constructing \hat{h}_2 . However, they can still be used to reduce the computational cost of \hat{h}_2 . And this is also the reason that only 63 evaluations to h_2 are needed but not like that as much as 175 for \hat{h}_1 . This advancement enables researchers to implement Bayesian updating with relatively small number of calls to the likelihood function.

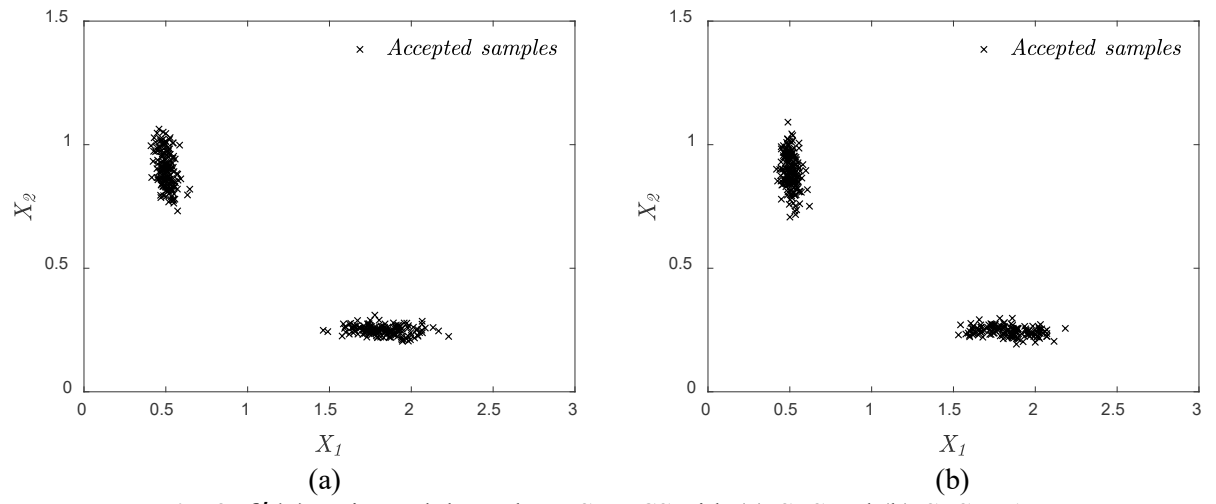


Fig. 8. f'(x) estimated through BUS+MCS with (a) SRS and (b) SRS-MARV.

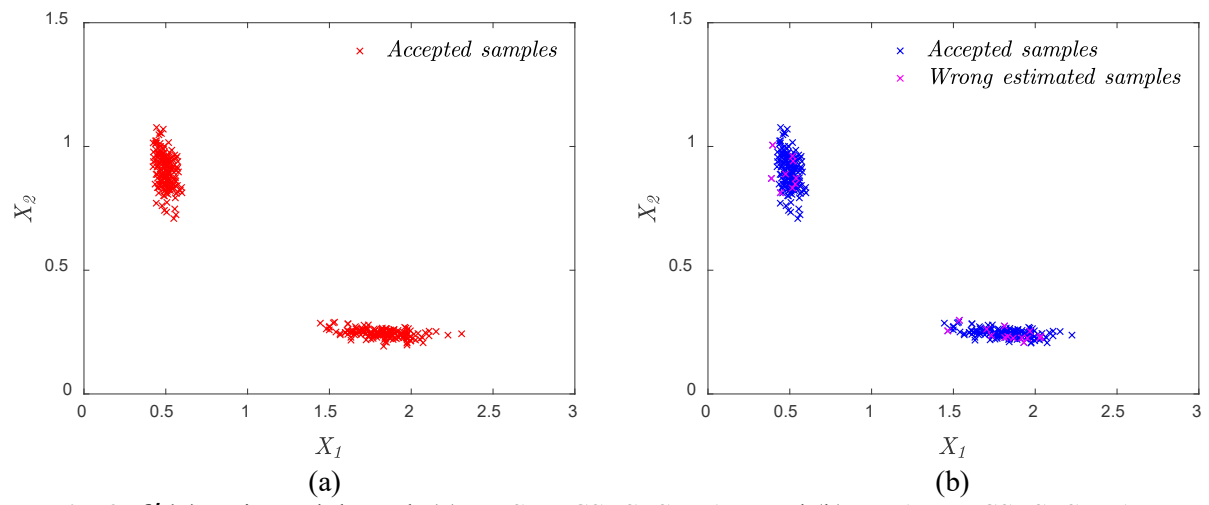


Fig. 9. f'(x) estimated through (a) BUS+MCS+SRS-MARV and (b) BUAK+MCS+SRS-MARV.

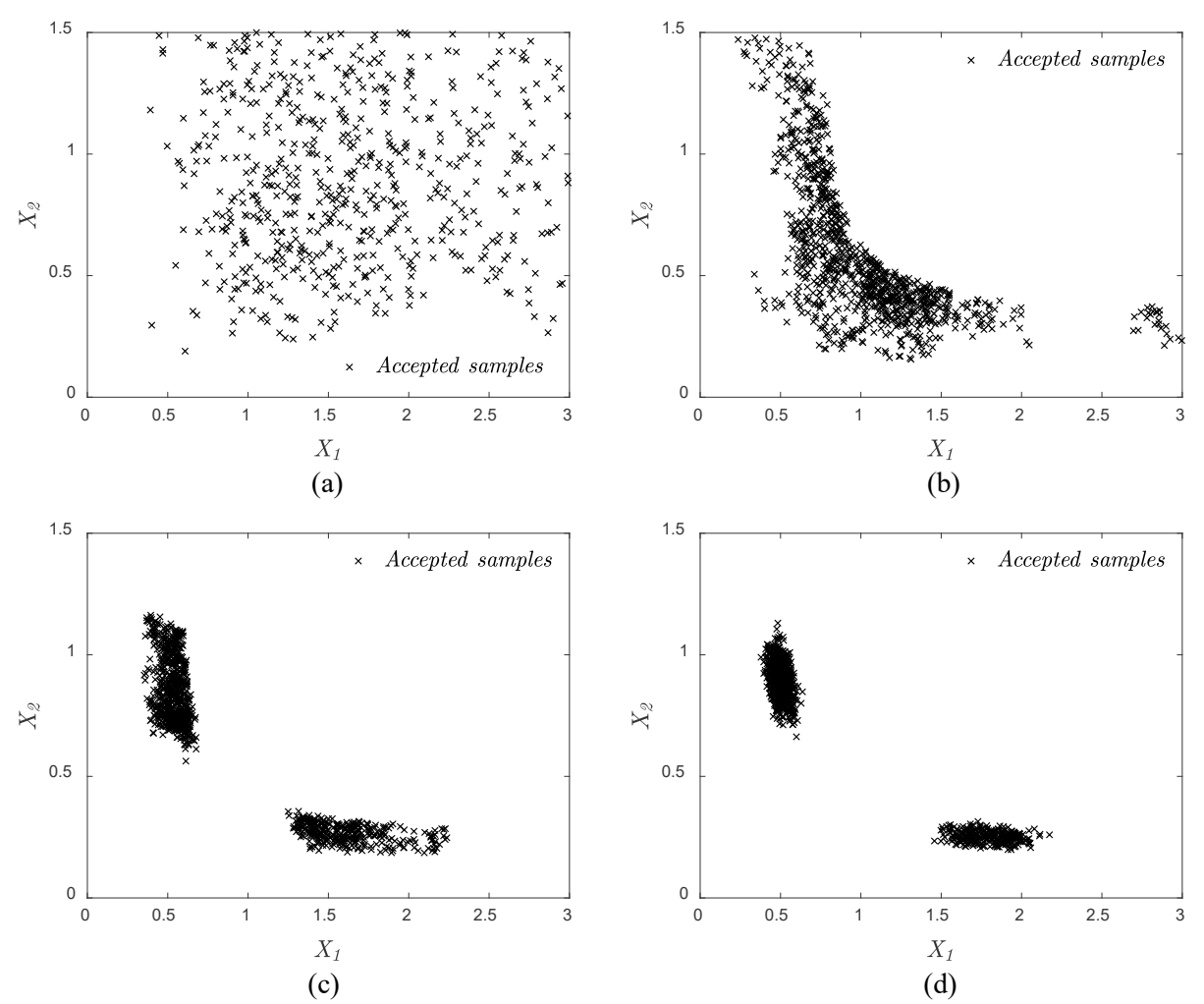


Fig. 10 Accepted samples using *BUS+SS+SRS-MARV* in (a) the first subset, (b) the second subset, (c) the third subset, and (d) the last subset.

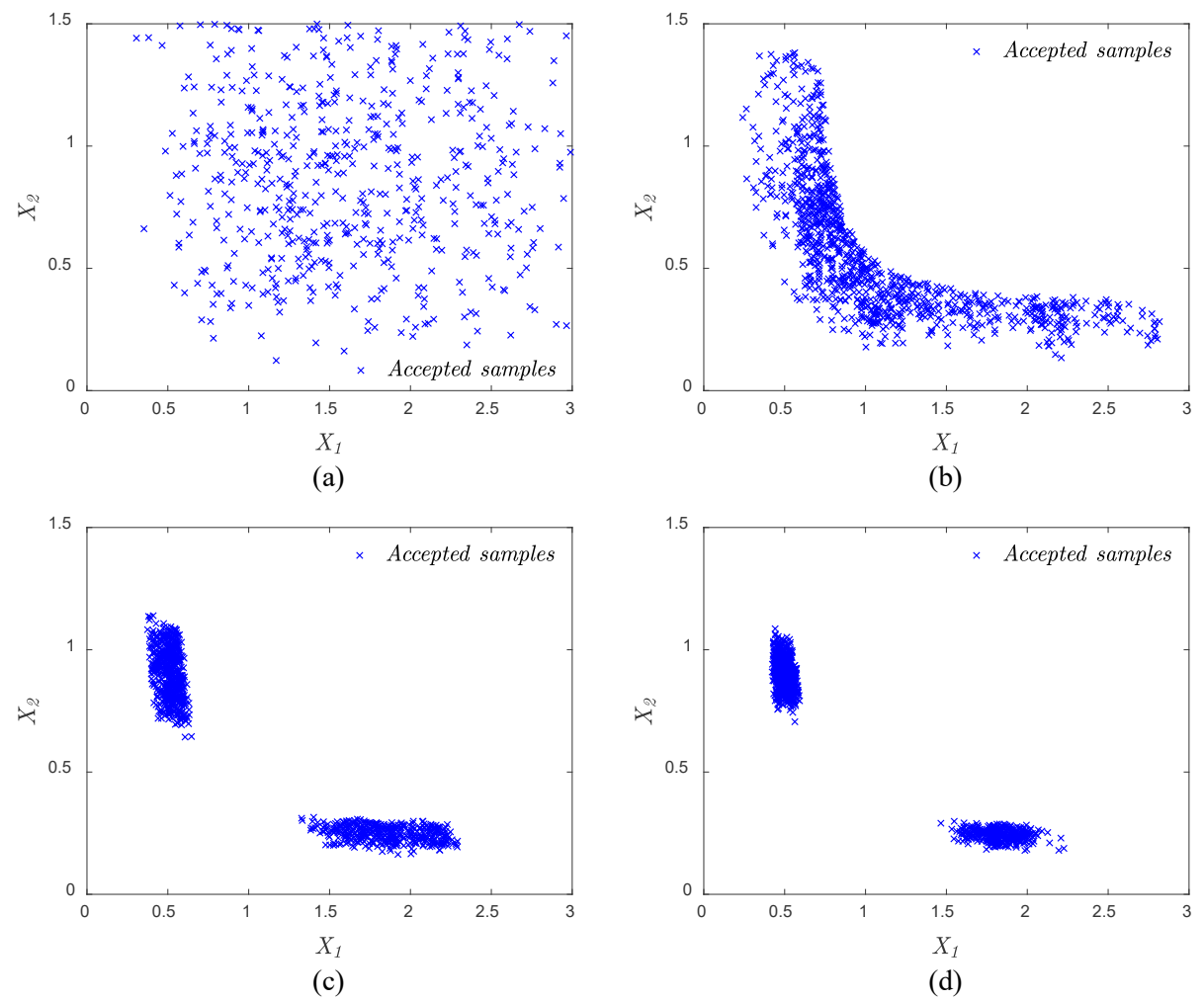


Fig. 11 Accepted samples using *BUAK+SS+SRS-MARV* in (a) the first subset, (b) the second subset, (c) the third subset, and (d) the last subset.

Table 7. Bayesian Updating results for example 3. $\hat{\mu}'(L)$, $\hat{\mu}'(R)$, $\hat{\sigma}'(L)$ and $\hat{\sigma}'(R)$ denote the estimated means(left and right cluster) and standard deviation(left and right cluster) for the posterior distribution f'(x). $\Psi_{thr} = 1 \times 10^{-3}$ is set in this case.

Methodology	Sampling method	N_{call}	$\hat{\mu}'(L)$	$\hat{\sigma}'(L)$	$\hat{\mu}'(R)$	$\hat{\sigma}'(R)$
BUS+MCS	SRS	2×10^{5}	0.5077	0.0421	1.8209	0.1412
BUS+MCS	SRS-MARV	2×10^5	0.4996	0.0406	1.8146	0.1544
BUS+SS	SRS-MARV	3758	0.5038	0.0407	1.8191	0.1476
BUAK+MCS	SRS-MARV	12 + 175 + 63	0.4997	0.0417	1.8093	0.1527
BUAK+SS	SRS-MARV	12 + 175 + 63	0.5032	0.0388	1.8197	0.1352

Table 8. Confusion matrix for the classification results using *BUAK+MCS+SRS-MARV*.

Actual	Predicted Class			
Class	Rejected	Accepted		
Rejected	199656	23		
Accepted	15	306		

For example 3, 100 simulations are conducted to investigate the average performance of the proposed method compared to the *BUS* approach. These simulation results are summarized in Table 9 and 10. For this case, the expected number of calls to the limit state function $E(N_{call})$, expected value of the estimated mean $E(\hat{\mu}')$ and standard deviation $E(\hat{\sigma}')$ on the left and right sides and their corresponding coefficients of variation (C.O.V) are recorded. According to Table 9 and 10, BUS + MCS is the most accurate approach with smallest variance. For example, the coefficients of variation of the mean of samples following the posterior distribution on the left and right sides are only 0.005 and 0.007, respectively, which are very small compared to other approaches. The application of subset simulation can increase the variance of the stochastic estimator. The proposed approach based on surrogate model can estimate the probabilistic properties of the samples with posterior distributions, however, with a slightly increased uncertainty. For instance, BUAK + MCS delivers $E(\hat{\mu}'(R)) = 1.816$ and $E(\hat{\sigma}'(R)) = 0.143$ with C.O.V of 0.012 and 0.122, respectively, while BUS + MCS yields $E(\hat{\mu}'(R)) = 1.817$ and $E(\hat{\sigma}'(R)) = 0.141$ with C.O.V of 0.007 and 0.069, respectively. However, the proposed BUAK approach only needs a very small number of calls to the performance function with $E(N_{call}) = 272.68$ compared to 2×10^5 for BUS + MCS.

Table 9. The performance of Bayesian Updating with 100 simulations for example 3 (On the left side).

Methodology	$E(N_{call})$	C.O.V (N_{call})	$E(\hat{\mu}'(L))$	$E(\hat{\sigma}'(L))$	C.O.V $(\hat{\mu}'(L))$	$C.O.V$ $(\hat{\sigma}'(L))$
BUS + MCS	2×10^{5}	-	0.502	0.038	0.005	0.050
BUAK + MCS	252.68	0.483	0.502	0.038	0.007	0.092
BUS + SS	3674.52	0.037	0.505	0.044	0.006	0.051
BUAK + SS	252.68	0.483	0.498	0.049	0.013	0.113

Table 10. The performance of Bayesian Updating with 100 simulations for example 3(On the right side).

Methodology	$E(\hat{\mu}'(R))$	$E(\hat{\sigma}'(R))$	C.O.V $(\hat{\mu}'(R))$	C.O.V $(\hat{\sigma}'(R))$
BUS + MCS	1.817	0.141	0.007	0.069
BUAK + MCS	1.816	0.143	0.012	0.122
BUS + SS	1.824	0.137	0.017	0.103
BUAK + SS	1.829	0.135	0.023	0.137

6. Conclusion

1

2

3

4

5

6

7

8

9

10

11

12

13

14

15

16

17

18

19

20

21

22

To enhance Bayesian updating techniques, a novel approach, called BUAK, is proposed in this paper that integrates Bayesian Updating with Structural reliability methods (BUS) with Adaptive Kriging surrogate modeling. Integration of BUS with advanced adaptive Kriging-based reliability analysis methods offers new capabilities in reducing the number of evaluations of costly performance functions and simultaneously training very accurate surrogate models. However, one of the challenging problems in implementing adaptive Kriging-based reliability analysis methods is the extremely small acceptance rate corresponding to the limit state function generated via BUS, as the number of observations increases. This leads to adaptive Kriging-based reliability analysis methods requiring significantly large numbers of candidate design samples to construct a refined limit state. Such a process can be computationally inefficient and is often not feasible. To address this limitation, the limit state function derived through BUS is decomposed into multiple sub-limit state functions with relatively large acceptance rates. Toward this goal, Simple Rejection Sampling with Multiple Auxiliary Random Variables (SRS-MARV) is proposed in this paper. By training multiple Kriging surrogates for these decomposed limit state functions, Bayesian updating can be well implemented using adaptive Kriging-based reliability analysis methods. Three numerical examples are investigated to examine the performance of the proposed method, BUAK. Results indicate that BUAK offers high accuracy in estimating the posterior distribution of random variables, while significantly reducing the number of evaluations of costly likelihood functions. However, BUAK has some limitations for highdimensional problems (e.g., known as the curse of dimensionality) due to the large computational demand associated with large matrix operations in constructing Kriging surrogate models. These limitations can hamper the application of BUAK for problems that have a large number of random inputs such as random field representations of spatially distributed properties. A potential solution is to control the number of candidate design samples via integration of the BUS+SS algorithm with adaptive Kriging.

24

25

26

23

Acknowledgments

This research has been partly funded by the U.S. National Science Foundation (NSF) through awards

- 1 CMMI-1563372, 1635569, and 1762918. Any opinions, findings, and conclusions or recommendations
- 2 expressed in this paper are those of the authors and do not necessarily reflect the views of the National
- 3 Science Foundation.

5

References

- 6 [1] Beck James L. and Au Siu-Kui, "Bayesian Updating of Structural Models and Reliability using
- 7 Markov Chain Monte Carlo Simulation," J. Eng. Mech., vol. 128, no. 4, pp. 380–391, Apr. 2002.
- 8 [2] Beck J. L. and Katafygiotis L. S., "Updating Models and Their Uncertainties. I: Bayesian Statistical
- 9 Framework," *J. Eng. Mech.*, vol. 124, no. 4, pp. 455–461, Apr. 1998.
- 10 [3] D. G. Giovanis, I. Papaioannou, D. Straub, and V. Papadopoulos, "Bayesian updating with subset
- simulation using artificial neural networks," Comput. Methods Appl. Mech. Eng., vol. 319, pp. 124–
- 12 145, Jun. 2017.
- 13 [4] Straub Daniel and Papaioannou Iason, "Bayesian Updating with Structural Reliability Methods," J.
- 14 Eng. Mech., vol. 141, no. 3, p. 04014134, Mar. 2015.
- 15 [5] W. Betz, I. Papaioannou, J. L. Beck, and D. Straub, "Bayesian inference with Subset Simulation:
- Strategies and improvements," *Comput. Methods Appl. Mech. Eng.*, vol. 331, pp. 72–93, Apr. 2018.
- 17 [6] Ching Jianye and Chen Yi-Chu, "Transitional Markov Chain Monte Carlo Method for Bayesian
- Model Updating, Model Class Selection, and Model Averaging," J. Eng. Mech., vol. 133, no. 7, pp.
- 19 816–832, Jul. 2007.
- 20 [7] Betz Wolfgang, Papaioannou Iason, and Straub Daniel, "Transitional Markov Chain Monte Carlo:
- 21 Observations and Improvements," *J. Eng. Mech.*, vol. 142, no. 5, p. 04016016, May 2016.
- 22 [8] S.-K. Au and J. L. Beck, "Estimation of small failure probabilities in high dimensions by subset
- simulation," *Probabilistic Eng. Mech.*, vol. 16, no. 4, pp. 263–277, 2001.
- 24 [9] S. K. Au and J. L. Beck, "Subset simulation and its application to seismic risk based on dynamic
- analysis," *J. Eng. Mech.*, vol. 129, no. 8, pp. 901–917, 2003.

- 1 [10] D. Straub, I. Papaioannou, and W. Betz, "Bayesian analysis of rare events," J. Comput. Phys., vol.
- 2 314, pp. 538–556, Jun. 2016.
- 3 [11] R. Schneider, S. Thöns, and D. Straub, "Reliability analysis and updating of deteriorating systems
- 4 with subset simulation," *Struct. Saf.*, vol. 64, pp. 20–36, Jan. 2017.
- 5 [12] S. Rahrovani, S.-K. Au, and T. Abrahamsson, "Bayesian Treatment of Spatially-Varying Parameter
- 6 Estimation Problems via Canonical BUS," in Model Validation and Uncertainty Quantification,
- 7 *Volume 3*, Springer, Cham, 2016, pp. 1–13.
- 8 [13] V. J. Romero, L. P. Swiler, and A. A. Giunta, "Construction of response surfaces based on
- 9 progressive-lattice-sampling experimental designs with application to uncertainty propagation,"
- 10 Struct. Saf., vol. 26, no. 2, pp. 201–219, 2004.
- 11 [14] W. Zhao, F. Fan, and W. Wang, "Non-linear partial least squares response surface method for
- structural reliability analysis," *Reliab. Eng. Syst. Saf.*, vol. 161, pp. 69–77, May 2017.
- 13 [15] G. Blatman and B. Sudret, "An adaptive algorithm to build up sparse polynomial chaos expansions
- for stochastic finite element analysis," *Probabilistic Eng. Mech.*, vol. 25, no. 2, pp. 183–197, 2010.
- 15 [16] H. Dai, H. Zhang, W. Wang, and G. Xue, "Structural reliability assessment by local approximation
- of limit state functions using adaptive Markov chain simulation and support vector regression,"
- 17 *Comput.-Aided Civ. Infrastruct. Eng.*, vol. 27, no. 9, pp. 676–686, 2012.
- 18 [17] J.-M. Bourinet, "Rare-event probability estimation with adaptive support vector regression surrogates,"
- 19 Reliab. Eng. Syst. Saf., vol. 150, pp. 210–221, 2016.
- 20 [18] B. Echard, N. Gayton, and M. Lemaire, "AK-MCS: an active learning reliability method combining
- 21 Kriging and Monte Carlo simulation," Struct. Saf., vol. 33, no. 2, pp. 145–154, 2011.
- 22 [19] W. Fauriat and N. Gayton, "AK-SYS: An adaptation of the AK-MCS method for system reliability,"
- 23 Reliab. Eng. Syst. Saf., vol. 123, pp. 137–144, 2014.
- 24 [20] Z. Wang and A. Shafieezadeh, "On confidence intervals for failure probability estimates in Kriging-
- based reliability analysis," *Reliab. Eng. Syst. Saf.*, vol. 196, p. 106758, Apr. 2020.

- 1 [21] M. Rahimi, A. Shafieezadeh, D. Wood, E. J. Kubatko, and N. C. Dormady, "Bayesian calibration of
- 2 multi-response systems via multivariate Kriging: Methodology and geological and geotechnical case
- 3 studies," *Eng. Geol.*, vol. 260, p. 105248, Oct. 2019.
- 4 [22] I. Kaymaz, "Application of kriging method to structural reliability problems," *Struct. Saf.*, vol. 27, no.
- 5 2, pp. 133–151, 2005.
- 6 [23] B. Gaspar, A. P. Teixeira, and C. G. Soares, "Assessment of the efficiency of Kriging surrogate
- 7 models for structural reliability analysis," *Probabilistic Eng. Mech.*, vol. 37, pp. 24–34, Jul. 2014.
- 8 [24] Rahimi Mehrzad, Wang Zeyu, Shafieezadeh Abdollah, Wood Dylan, and Kubatko Ethan J., "An
- 9 Adaptive Kriging-Based Approach with Weakly Stationary Random Fields for Soil Slope Reliability
- 10 Analysis," *Geo-Congr. 2019*, pp. 148–157.
- 11 [25] Z. Wang and A. Shafieezadeh, "REAK: Reliability analysis through Error rate-based Adaptive
- 12 Kriging," *Reliab. Eng. Syst. Saf.*, vol. 182, pp. 33–45, Feb. 2019.
- 13 [26] Z. Wang and A. Shafieezadeh, "Real-time high-fidelity reliability updating with equality information
- using adaptive Kriging," Reliab. Eng. Syst. Saf., vol. 195, p. 106735, Mar. 2020.
- 15 [27] W. Betz, J. L. Beck, I. Papaioannou, and D. Straub, "Bayesian inference with reliability methods
- without knowing the maximum of the likelihood function," *Probabilistic Eng. Mech.*, vol. 53, pp. 14–
- 17 22, Jun. 2018.
- 18 [28] A. F. M. Smith and A. E. Gelfand, "Bayesian Statistics without Tears: A Sampling-Resampling
- 19 Perspective," *Am. Stat.*, vol. 46, no. 2, pp. 84–88, May 1992.
- 20 [29] "UQLab Kriging (Gaussian process modelling) manual," UQLab, the Framework for Uncertainty
- 21 Quantification. [Online]. Available: http://www.uqlab.com/userguidekriging. [Accessed: 13-May-
- 22 2017].
- 23 [30] "UQLab sensitivity analysis user manual," UQLab, the Framework for Uncertainty Quantification.
- [Online]. Available: http://www.uqlab.com/userguide-reliability. [Accessed: 13-May-2017].

- 1 [31] B. Echard, N. Gayton, M. Lemaire, and N. Relun, "A combined importance sampling and kriging
- 2 reliability method for small failure probabilities with time-demanding numerical models," *Reliab*.
- 3 Eng. Syst. Saf., vol. 111, pp. 232–240, 2013.
- 4 [32] X. Huang, J. Chen, and H. Zhu, "Assessing small failure probabilities by AK–SS: an active learning
- 5 method combining Kriging and subset simulation," *Struct. Saf.*, vol. 59, pp. 86–95, 2016.
- 6 [33] Z. Hu and X. Du, "Mixed Efficient Global Optimization for Time-Dependent Reliability Analysis,"
- 7 *J. Mech. Des.*, vol. 137, no. 5, pp. 051401-051401–9, May 2015.
- 8 [34] S. N. Lophaven, H. B. Nielsen, and J. Søndergaard, "DACE-A Matlab Kriging toolbox, version 2.0,"
- 9 2002.

- 10 [35] J. Wang, Z. Sun, Q. Yang, and R. Li, "Two accuracy measures of the Kriging model for structural
- reliability analysis," *Reliab. Eng. Syst. Saf.*, vol. 167, pp. 494–505, Nov. 2017.
- 12 [36] Z. Wen, H. Pei, H. Liu, and Z. Yue, "A Sequential Kriging reliability analysis method with
- characteristics of adaptive sampling regions and parallelizability," *Reliab. Eng. Syst. Saf.*, vol. 153,
- pp. 170–179, 2016.
- 15 [37] W. Betz, I. Papaioannou, and D. Straub, "Adaptive variant of the BUS approach to Bayesian updating,"
- presented at the EURODYN 2014, 2014.